

# BIJECTIVE PROOFS FOR SCHUR FUNCTION IDENTITIES

MARKUS FULMEK

ABSTRACT. In [4], Gurevich, Pyatov and Saponov stated an expansion for the product of two Schur functions and gave a proof based on the Plücker relations.

Here we show that this identity is in fact a special case of a quite general Schur function identity, which was stated and proved in [1, Lemma 16]. In [1], it was used to prove bijectively Dodgson’s condensation formula and the Plücker relations, but was not paid further attention: So we take this opportunity to make obvious the range of applicability of this identity by giving concrete examples, accompanied by many graphical illustrations.

## 1. INTRODUCTION

In [4], Gurevich, Pyatov and Saponov stated an expansion for the product of two Schur functions and gave a proof based on the Plücker relations. Here we show that this identity is in fact a special case of a more general Schur function identity [1, Lemma 16]. Since this involves a process of “translation” between the languages of [1] and [4] which might not be self-evident, we explain again the corresponding combinatorial constructions here. These constructions are best conceived by pictures, so we give a lot of figures illustrating the concepts.

This paper is organized as follows:

In Section 2 we recall the basic definitions (partitions, Young tableaux, skew Schur functions and nonintersecting lattice paths).

In Section 3, we present the central bijective construction (recolouring of bicoloured paths in the overlays of families of nonintersecting lattice paths corresponding to some product of skew Schur functions) and show how this yields a quite general Schur function identity (Theorem 1, a reformulation of [1, Lemma 16]).

In Section 4 we try to exhibit the broad range of applications of Theorem 1: In particular, we show how the identity [4, (3.3)] appears as (a translation of) a special case of Theorem 1.

## 2. BASIC DEFINITIONS

An infinite weakly decreasing series of nonnegative integers  $(\lambda_i)_{i=1}^{\infty}$ , where only finitely many elements are positive, is called a *partition*. The largest index  $i$  for which  $\lambda_i > 0$  is

---

*Date:* November 21, 2018.

Research supported by the National Research Network “Analytic Combinatorics and Probabilistic Number Theory”, funded by the Austrian Science Foundation.

called the *length* of the partition  $\lambda$  and is denoted by  $\ell(\lambda)$ . For convenience, we shall in most cases omit the trailing zeroes, i.e., for  $\ell(\lambda) = r$  we simply write  $\lambda = (\lambda_1, \lambda_2, \dots, \lambda_r)$ , where  $\lambda_1 \geq \lambda_2 \geq \dots \geq \lambda_r > 0$ .

The *Ferrers diagram*  $F_\lambda$  of  $\lambda$  is an array of cells with  $\ell(\lambda)$  left-justified rows and  $\lambda_i$  cells in row  $i$ .

An  *$N$ -semistandard Young tableau* of shape  $\lambda$  is a filling of the cells of  $F_\lambda$  with integers from the set  $\{1, 2, \dots, N\}$ , such that the numbers filled into the cells weakly increase in rows and strictly increase in columns.

Let  $T$  be a semistandard Young tableau and define  $m(T, k)$  to be the number of entries  $k$  in  $T$ . Then the weight  $w(T)$  of  $T$  is defined as follows:

$$\omega(T) = \prod_{k=1}^N x_k^{m(T, k)}.$$

*Schur functions*, which are irreducible general linear characters, can be combinatorially defined by means of  $N$ -semistandard Young tableaux (see, for instance, [5, Definition 4.4.1]):

$$s_\lambda(x_1, x_2, x_3, \dots, x_N) = \sum_T \omega(T),$$

where the sum is over all  $N$ -semistandard Young tableaux  $T$  of shape  $\lambda$ .

Consider some partition  $\lambda = (\lambda_1, \dots, \lambda_r > 0)$ , and let  $\mu$  be a partition such that  $\mu_i \leq \lambda_i$  for all  $i \geq 1$ . The *skew Ferrers diagram*  $F_{\lambda/\mu}$  of  $\lambda/\mu$  is an array of cells with  $r$  left-justified rows and  $\lambda_i - \mu_i$  cells in row  $i$ , where the first  $\mu_i$  cells in row  $i$  are missing. An  *$N$ -semistandard skew Young tableau* of shape  $\lambda/\mu$  is a filling of the cells of  $F_{\lambda/\mu}$  with integers from the set  $\{1, 2, \dots, N\}$ , such that the numbers filled into the cells weakly increase in rows and strictly increase in columns (see the left picture of Figure 1 for an illustration).

Then we can define the *skew Schur function*:

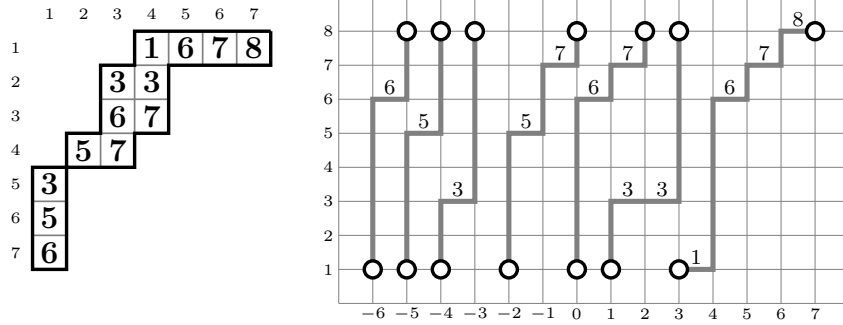
$$s_{\lambda/\mu}(x_1, x_2, x_3, \dots, x_N) = \sum_T \omega(T), \tag{1}$$

where the sum is over all  $N$ -semistandard skew Young tableaux  $T$  of shape  $\lambda/\mu$ , where the weight  $\omega(T)$  of  $T$  is defined as before.

Note that for  $\mu = (0, 0, \dots)$  the skew Schur function  $s_{\lambda/\mu}$  is identical to the “ordinary” Schur function  $s_\lambda$ .

The Gessel-Viennot interpretation [2] gives an equivalent description of a semistandard Young tableau  $T$  of shape  $\lambda/\mu$  as an  $r$ -tuple  $P = (p_1, \dots, p_r)$  of nonintersecting lattice paths, where  $r := \ell(\lambda)$ : Fix some (arbitrary) integer *shift*  $t$  and consider paths in the lattice  $\mathbb{Z}^2$  (i.e., in the directed graph with vertices  $\mathbb{Z} \times \mathbb{Z}$  and arcs from  $(j, k)$  to  $(j+1, k)$  and from  $(j, k)$  to  $(j, k+1)$  for all  $j, k$ ). The  $i$ -th path  $p_i$  starts at  $(\mu_i - i + t, 1)$  and ends at  $(\lambda_i - i + t, N)$ , and the  $j$ -th *horizontal* step in  $p_i$  goes from  $(-i + t + j - 1, h)$

FIGURE 1. The left picture presents a semistandard Young tableau  $T$  of skew shape  $\lambda/\mu$ , where  $\lambda = (7, 4, 4, 3, 1, 1, 1)$  and  $\mu = (3, 2, 2, 1)$ . Assuming that the entries of  $T$  are chosen from  $\{1, 2, \dots, 8\}$  (i.e.:  $T$  is an 8-semistandard Young tableau), the right picture shows the corresponding family of  $7 = \ell(\lambda)$  nonintersecting lattice paths (with shift  $t = 0$ ): Note that the height of the  $j$ -th horizontal step in the  $i$ -th path (the paths are counted from right to left) is equal to the  $j$ -th entry in row  $i$  of  $T$ .



to  $(-i + t + j, h)$ , where  $h$  is the  $j$ -th entry in row  $i$  of  $T$ . Note that the conditions on the entries of  $T$  imply that no two paths  $p_i$  and  $p_j$  thus defined have a lattice point in common: such an  $r$ -tuple of paths is called *nonintersecting* (see the right picture of Figure 1 for an illustration).

In fact, this translation of tableaux to nonintersecting lattice paths is a *bijection* between the set of all  $N$ -semistandard Young tableaux of shape  $\lambda/\mu$  and the set of all  $r$ -tuples of nonintersecting lattice paths with starting and ending points as defined above. This bijection is *weight preserving* if we define the weight of an  $r$ -tuple  $P$  of nonintersecting lattice paths in the obvious way, i.e., as

$$\omega(P) := \prod_{k=1}^N x_k^{n(P,k)},$$

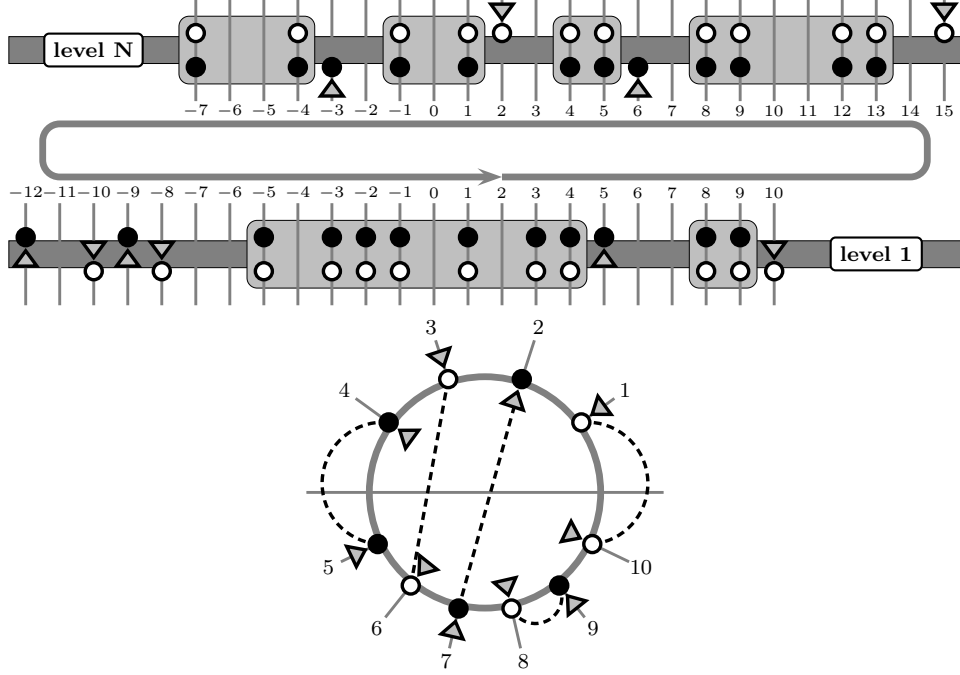
where  $n(P, k)$  is the number of horizontal steps at height  $k$  in  $P$ . So in the definition (1) we could equivalently replace symbol “ $T$ ” by symbol “ $P$ ”, and sum over  $r$ -tuples of lattice paths with prescribed starting and ending points instead of tableaux with prescribed shape.

Note that the horizontal coordinates of starting and ending points determine uniquely the *shape*  $\lambda/\mu$  of the tableau, and the vertical coordinate (we shall call the vertical coordinate of points the *level* in the following) of the ending points determines uniquely the *set of entries*  $\{1, 2, \dots, N\}$  of the tableau. (The choice of the shift parameter  $t$  does influence neither the shape nor the set of entries.)

### 3. BICOLOURED PATHS AND PRODUCTS OF SKEW SCHUR FUNCTIONS

In the following, all skew Schur functions are considered as functions of the variables  $(x_1, \dots, x_N)$ . (Equivalently, all tableaux have entries from the set  $\{1, \dots, N\}$ , and all families of nonintersecting lattice paths have ending points on level  $N$ ).

FIGURE 2. Illustration for the example given in Section 3.



Viewing the product of two skew Schur functions

$$s_{\lambda/\mu} \cdot s_{\sigma/\tau}$$

as the generating function of “overlays of two families of nonintersecting lattice paths” (according to definition (1)) gives rise to a bijective construction, which (to the best of our knowledge) was first used by Goulden [3]. This construction was used in [1] to describe and prove a class of Schur function identities, special cases of which imply Dodgson’s condensation formula and the Plücker relations.

We shall present this construction by way of an example: Consider skew shapes  $\lambda/\mu$ , where

$$\begin{aligned} \lambda &= (14, 13, 13, 11, 11, 9, 9, 8, 8, 7, 5, 3), \\ \mu &= (9, 9, 9, 6, 6, 5, 4, 4, 4, 3, 1), \end{aligned} \tag{2}$$

and  $\sigma/\tau$ , where

$$\begin{aligned} \sigma &= (14, 14, 12, 12, 11, 11, 11, 9, 8, 7, 7, 5), \\ \tau &= (10, 10, 8, 8, 8, 7, 6, 6, 6, 5, 2). \end{aligned} \tag{3}$$

For the skew shape  $\lambda/\mu$ , choose fixed shift 2, and for the skew shape  $\sigma/\tau$  choose fixed shift 0, and consider the starting and ending points of the corresponding families of nonintersecting lattice paths. For instance, the ending point of the first path corresponding to  $\lambda/\mu$  is  $(\lambda_1 - 1 + 2, N) = (15, N)$ , and the starting point of the last (twelfth) path corresponding to  $\lambda/\mu$  is  $(\mu_{12} - 12 + 2, 1) = (-10, 1)$ , and the ending point of the first path corresponding to  $\sigma/\tau$  is  $(\sigma_1 - 1, N) = (13, N)$ .

Now colour the starting/ending points corresponding to  $\lambda/\mu$  *white*, and the starting/ending points corresponding to  $\sigma/\tau$  *black*: See the upper picture of Figure 2, where

the starting/ending points of  $\lambda/\mu$  are drawn as white circles, and the starting/ending points of  $\sigma/\tau$  are drawn as black circles.

All starting/ending points which are coloured both black *and* white are never affected by the following constructions: In the upper picture of Figure 2, these points are enclosed by grey rectangles.

We call the remaining starting/ending points (which are coloured *either* black *or* white) the *coloured* points. Note that the number of coloured points is necessarily *even*.

For the coloured points, assume the circular orientation “from right to left along level  $N$ , and then from left to right along level 1”. In the upper picture of Figure 2, this circular orientation is indicated by a grey circular arrow.

Furthermore, assign to paths corresponding to  $\lambda/\mu$  the orientation *downwards*, and to paths corresponding to  $\sigma/\tau$  the orientation *upwards*. In the upper picture of Figure 2, this orientation of paths is indicated by upwards or downwards pointing triangles.

If we focus on the coloured points, we may encode the situation in a simpler picture, where the coloured starting/ending points are located on the lower/upper half of a *circle*, and where the orientation of the respective path is translated to a *radial orientation* (either towards the center of the circle or away from it). The lower picture of Figure 2 illustrates this: A grey horizontal line indicates the separation of the lower and upper half of the circle, the point labeled 1 corresponds to the lattice point  $(15, N)$ , the point labeled 2 corresponds to the lattice point  $(6, N)$ , and so on.

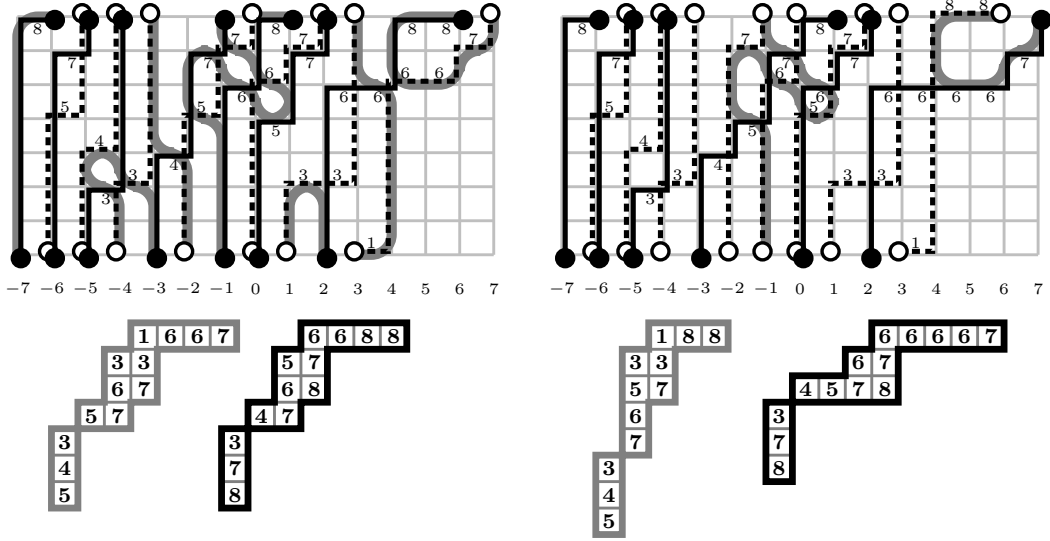
Now consider some pair  $(P_1, P_2)$  of families of nonintersecting lattice paths, where  $P_1$  corresponds to some tableau of shape  $\lambda/\mu$ , and  $P_2$  corresponds to some tableau of shape  $\sigma/\tau$ . We call the paths of  $P_1$  the *white* paths and the paths of  $P_2$  the *black* paths, and we colour the arcs of the lattice  $\mathbb{Z}^2$  accordingly (i.e., arcs used by some white path are coloured white, and arcs used by some black path are coloured black). As with the starting/ending points, arcs which are coloured black *and* white are not affected by the following construction, and we call all arcs which are *either* black *or* white the *coloured* arcs. We construct *bicoloured paths*

- connecting (only) coloured starting/ending points
- and using (only) coloured arcs

by the following algorithm:

We start at some coloured point  $q$  and follow the path determined by the *unique* coloured arc incident with it in the respective orientation (i.e., either up/right or down/left). Whenever we meet *another* path on our way (necessarily, this path is of the other colour), we “change colour and orientation”, i.e., we follow this new path *and* change the orientation (i.e., if we were moving up/right along the old path, we move down/left along the new path, and vice versa). We stop if there is no possibility to go further.

FIGURE 3. The left picture presents two tableaux of the identical shape  $(7, 4, 4, 3, 1, 1, 1) / (3, 2, 2, 1)$  in the lower part, the upper part shows the corresponding overlay of black and white paths (white paths are indicated by dashed lines) and *all* bicoloured paths (indicated by thick grey lines). The right picture presents two tableaux of shapes  $(5, 3, 3, 2, 2, 1, 1, 1) / (2, 1, 1, 1, 1)$  and  $(9, 5, 5, 1, 1, 1) / (4, 3, 1)$ , respectively, in the lower part: These tableaux correspond to the overlay of lattice paths in the upper part, which is obtained by *recolouring* the bicoloured paths starting in  $(7, 8)$  and in  $(-1, 1)$  (these bicoloured paths are indicated by thick grey lines, again).



This construction is described in detail in [1]. Here, we simply refer to the left picture of Figure 3, where the white paths are indicated by dashed lines, and all bicoloured paths are indicated by thick grey lines.

The following observations are immediate:

**Observation 1 (Bicoloured paths always exist).** For *every* coloured point  $q$ , there exists a bicoloured path starting at  $q$ .

**Observation 2 (Bicoloured paths connect points of different radial orientation).** The bicoloured paths thus constructed never connect points of the same radial orientation (i.e., two points oriented both towards or both away from the center).

In the lower picture of Figure 2, a possible pattern of “connections by bicoloured paths” is indicated by dashed lines.

The following observation is easy to see:

**Observation 3 (Bicoloured path connect points of different parity).** Two different bicoloured paths may have lattice points in common (they may intersect), but they can never *cross*. If we assume some consecutive numbering of the coloured points in their circular orientation (see the lower picture of Figure 2), then this non-crossing condition

implies that there can never be a bicoloured path connecting two points with numbers of the same parity.

The non-crossing condition means that if all such connections were drawn as straight lines connecting points on the circle, then no two such lines can intersect. (In Figure 2, not all connections are drawn as straight lines for graphical reasons.)

Consider some bicoloured path  $b$  in the overlay of nonintersecting lattice paths  $(P_1, P_2)$ : Changing colours (black to white and vice versa)

- of both ending points of  $b$
- and of all arcs of  $b$

gives a new overlay of nonintersecting lattice paths  $(P'_1, P'_2)$  (with different starting/ending points). It is easy to see that we have for this *recolouring* of a bicoloured path:

**Observation 4 (Recolouring bicoloured paths is a weight preserving involution).** The recolouring of a bicoloured path  $b$  in an overlay of nonintersecting lattice paths  $(P_1, P_2)$  is an *involution operation* (i.e., if we obtain the overlay  $(P'_1, P'_2)$  by recolouring  $b$  in  $(P_1, P_2)$ , then recolouring  $b$  again in  $(P'_1, P'_2)$  yields the original  $(P_1, P_2)$ ), which *preserves the respective weights*, i.e.,

$$\omega(P_1) \cdot \omega(P_2) = \omega(P'_1) \cdot \omega(P'_2).$$

Return to the example illustrated in Figure 2 and consider the white ending point  $(15, N)$  and the black starting point  $(5, 1)$  there. Note that both of these points are marked with a triangle pointing *downward*. The bicoloured paths ending at these points must have their other ending points marked with a triangle pointing *upward*. One possible choice of these other ending points is depicted in Figure 4: The corresponding ending points are marked by white rectangles, the bicoloured paths are indicated by arrows. The picture shows the situation *after* recolouring these paths.

The skew shape corresponding to the white points in Figure 4 is  $\lambda'/\mu'$ , where

$$\begin{aligned} \lambda' &= (13, 13, 11, 11, 9, 9, 8, 8, 7, 5, 3), \\ \mu' &= (9, 9, 7, 7, 7, 6, 5, 5, 5, 4, 0). \end{aligned} \tag{4}$$

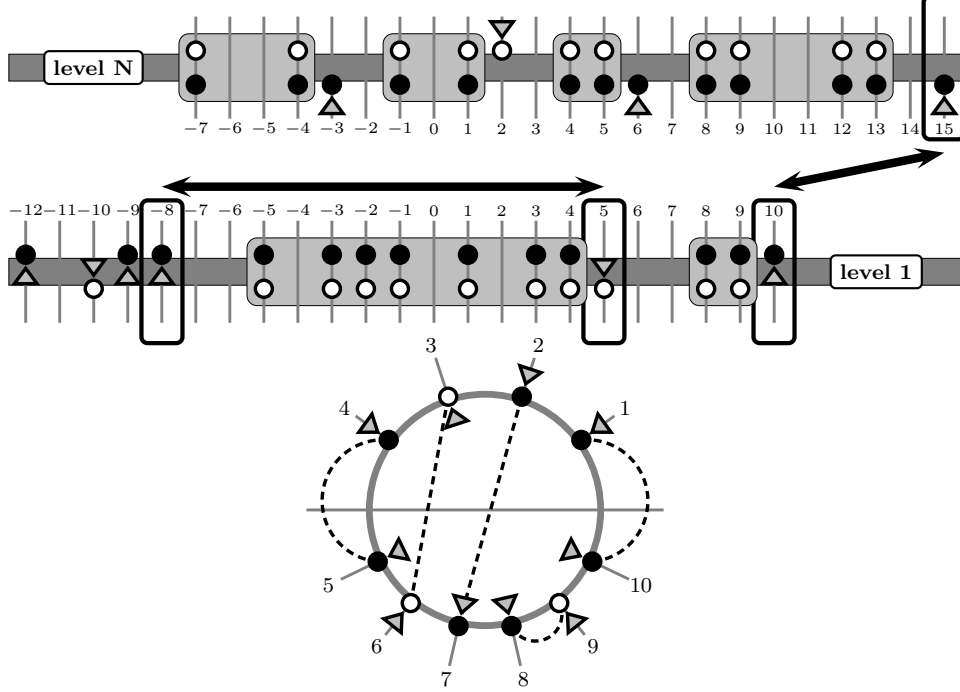
The skew shape corresponding to the black points in Figure 4 is  $\sigma'/\tau'$ , where

$$\begin{aligned} \sigma' &= (15, 14, 14, 12, 12, 11, 11, 11, 9, 8, 7, 7, 5), \\ \tau' &= (10, 10, 10, 7, 7, 6, 5, 5, 5, 4, 2, 2, 0). \end{aligned} \tag{5}$$

For both skew shapes, the starting and ending points are shifted by 1, so, for instance, the starting point of the first path corresponding to  $\sigma'/\tau'$  is  $(\tau'_1 - 1 + 1, 1) = (10, 1)$  and the ending point of the last (eleventh) path corresponding to  $\lambda'/\mu'$  is  $(\lambda'_{11} - 11 + 1, N) = (-7, N)$ .

The pictures in Figure 4 contain redundant information: All uncoloured points are “doubled”, and the colour (black or white) of the coloured points is determined uniquely by their circular orientation. So we may encode the information in a more terse way, namely as

FIGURE 4. The two (necessarily different, by Observation 2!) bicoloured paths in Figure 2 which start at the white ending point  $(15, N)$  and at the the black starting point  $(5, 1)$  may have their respective other ending points in  $(10, 1)$  and  $(-8, 1)$ . In the picture below, the corresponding points are marked by white rectangles, the bicoloured paths are indicated by arrows. The picture shows the situation *after* recolouring these paths.

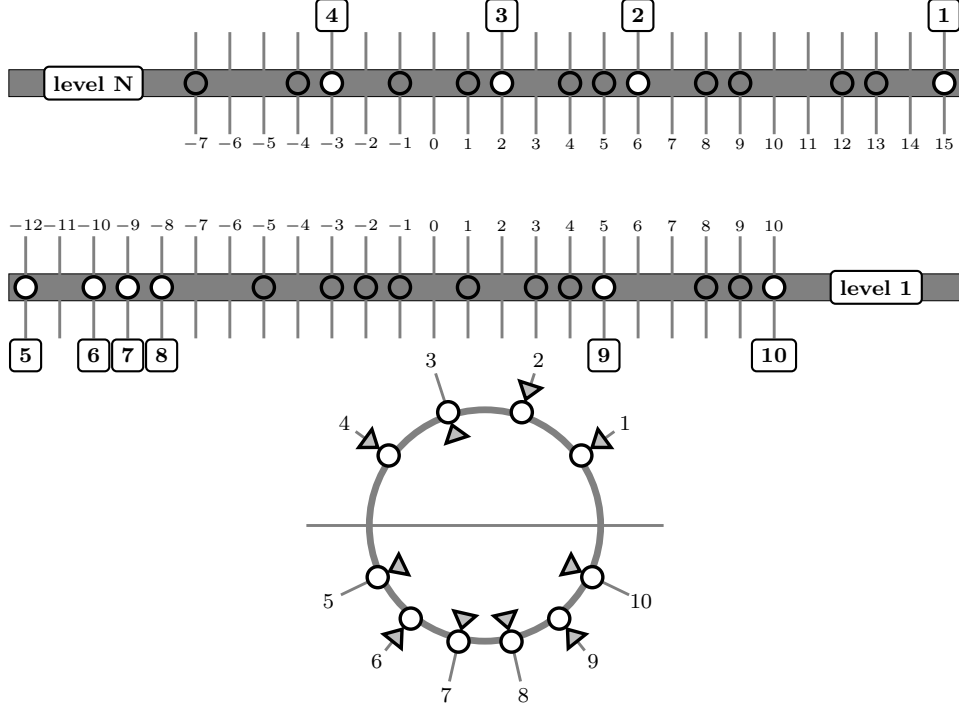


- the *configuration of (starting/ending) points* (short: **cp**) (see the upper picture in Figure 5),
- and the *circular orientation of coloured (starting/ending) points* (short: **cocp**) (see the lower picture in Figure 5).

We call a **cocp** *admissible* if it has the same number of inwardly/outwardly oriented points. *Every* admissible **cocp** determines (together with the corresponding **cp**) a certain configuration of starting/ending points. However, there might be no overlay of families of nonintersecting lattice paths that connect these points (if, for instance, the  $i$ -th white ending point lies to the left of the  $i$ -th white starting point; this would correspond to an  $i$ -th row of length  $< 0$  in the corresponding shape): In this case, the corresponding skew Schur function is zero. But if there *is* an overlay of families of nonintersecting lattice paths that connect these points, then the family of all bicoloured paths determines a *perfect matching*  $M$  in the **cocp** (according to Observation 1), which is *non-crossing* (according to Observation 3), and where all edges of  $M$  connect points of different radial orientation (according to Observation 2): We call such matchings *admissible*. Note that recolouring some bicoloured path amounts to reversing the orientation of the corresponding edge in the matching  $M$ .

We may summarize all these considerations as follows (this is a reformulation of [1, Lemma 15]):

FIGURE 5. The information of Figure 4 can be encoded in a more terse way, namely as the **cp** (shown in the upper picture) and the **cocp** (shown in the lower picture): The grey points in the upper picture are “doubled” points (coloured black *and* white), and the colour of the white points in the upper picture is determined by the *orientation* of the corresponding points in the lower picture (points in the upper half which are inwardly orientated and points in the lower half which are outwardly oriented should be coloured black; all other points should be coloured white).



**Lemma 1.** Let  $\lambda/\mu$  and  $\sigma/\tau$  be two skew shapes, and let  $t$  be an arbitrary integer. Consider the **cp** corresponding to the starting/ending points with shift 0 for  $\lambda/\mu$  and shift  $t$  for  $\sigma/\tau$ . In the corresponding **cocp**, choose a nonempty subset  $S$  (arbitrary, but fixed) of the points oriented towards the center.

Consider the set  $V$  of all admissible **cocps**, and consider the graph  $G$  with vertex set  $V$ , where two vertices  $v_1, v_2$  are connected by an edge if and only if there are overlays of lattice paths  $(P_1, P_2)$  and  $(P'_1, P'_2)$  for the starting/ending points corresponding to  $(\mathbf{cp}, v_1)$  and  $(\mathbf{cp}, v_2)$ , respectively, such that  $(P'_1, P'_2)$  is obtained from  $(P_1, P_2)$  by recolouring all bicoloured paths that are incident with some point of  $S$ .

Obviously, this graph  $G$  is bipartite (i.e.,  $V = E \cup O$  with  $E \cap O = \emptyset$ , such that there is no edge connecting two vertices of  $E$  or two vertices of  $O$ ).

Let  $C$  be an arbitrary connected component of  $G$  with at least 2 vertices, and denote by  $C_O$  the set of pairs of skew shapes corresponding to  $(\mathbf{cp}, x)$  for  $x \in O$ , and by  $C_E$  the set of pairs of skew shapes corresponding to  $(\mathbf{cp}, x)$  for  $x \in E$ . Then we have the following

identity for skew Schur functions:

$$\sum_{(\lambda/\mu, \sigma/\tau) \in C_E} s_{\lambda/\mu} \cdot s_{\sigma/\tau} = \sum_{(\lambda'/\mu', \sigma'/\tau') \in C_O} s_{\lambda'/\mu'} \cdot s_{\sigma'/\tau'}. \quad (6)$$

This Lemma is rather unwieldy. But there is a particularly simple situation which appears to be useful, so we state it as a Theorem (this is a reformulation of [1, Lemma 16]):

**Theorem 1.** *Under the assumptions of Lemma 1, let  $c$  be the **cocp** for the pair of shapes  $(\lambda/\mu, \sigma/\tau)$ , and assume that the orientation of the points in  $c$  is alternating. As in Lemma 1, let  $S$  be some fixed subset of the points oriented towards the center in  $c$ .*

*Consider the set of all **cocps** which can be obtained by reorienting all edges incident with points in  $S$  in some admissible matching of  $c$ , and denote the set of pairs of skew shapes corresponding to such **cocps** by  $Q$ .*

*Then we have:*

$$s_{\lambda/\mu} \cdot s_{\sigma/\tau} = \sum_{(\lambda'/\mu', \sigma'/\tau') \in Q} s_{\lambda'/\mu'} \cdot s_{\sigma'/\tau'}. \quad (7)$$

*Proof.* Observe that in the right hand side of (7) the Schur function product  $s_{\lambda'/\mu'} \cdot s_{\sigma'/\tau'}$  is either zero (if there is, in fact, no overlay of families of nonintersecting lattice paths corresponding to the respective **cocp**), or there is some corresponding overlay of families of nonintersecting lattice paths  $(P'_1, P'_2)$ . In the latter case, there *are* bicoloured paths starting in the points of  $S$  (by Observation 1), and by the combination of Observations 2 and 3, recolouring all such paths necessarily yields an overlay  $(P_1, P_2)$  of nonintersecting lattice paths which corresponds to the pair  $(\lambda/\mu, \sigma/\tau)$ .  $\square$

#### 4. APPLICATIONS

Clearly, the interpretation of Schur functions as generating functions of  $r$ -tuples of nonintersecting lattice paths is best suited for the bijective construction of recolouring bicoloured paths. But of course, the recolouring operation can be translated into operations for the shapes of the corresponding tableau (i.e., for the corresponding partitions, or equivalently, Ferrers diagrams).

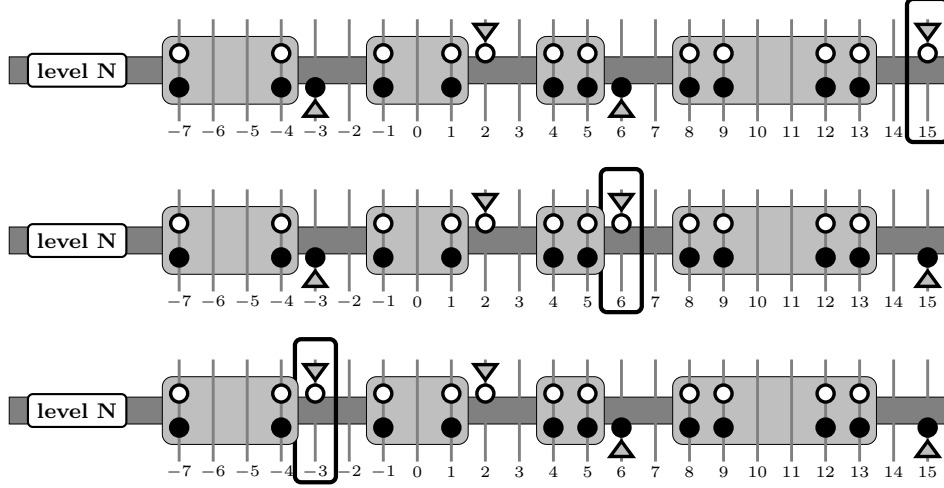
We shall show how this translation gives the identity [4, (3.3)] of Gurevich, Pyatov and Saponov, but before doing this we consider a simple special case, in order to illustrate the meaning of Theorem 1:

**Example 1.** *Assume that for the shapes  $\lambda/\mu$  and  $\sigma/\tau$  we have*

- $\mu = \tau$ ,
- $\lambda_1 > \sigma_1$ ,
- $\ell(\lambda) = \ell(\sigma)$ .

*Choose shift 0 for the families of starting/ending points corresponding to these shapes, then there is no coloured starting point (since  $\mu = \tau$ ): accordingly, only the ending points are shown in Figure 6. Furthermore, assume that the corresponding black and white ending points alternate along level  $N$ : Then the preconditions of Theorem 1 are fulfilled.*

FIGURE 6. Application of Lemma 1 to the special case  $\mu = \tau$ ,  $\lambda_1 > \sigma_1$ ,  $\ell(\lambda) = \ell(\sigma)$ , and shift 0 for *all* starting/ending points: Since there is no coloured starting point in this case, only the ending points (on level  $N$ ) are shown. The point  $(15, N)$  (ending point of bicoloured path  $b$ ) is marked with a white rectangle in the upper row. The middle row and the lower row show the configurations which can arise by recolouring  $b$ ; the respective other ending points  $(6, N)$  and  $(-3, N)$  are again marked with a white rectangle.



Since  $\lambda_1 > \mu_1$ , the point  $q = (\lambda_1 - 1, N)$  is white. Consider the set  $S = \{q\}$ : The bicoloured path  $b$  starting in  $q$  necessarily must end in a black point (by Observation 2). Assume that there are  $k$  such black points  $q_1, \dots, q_n$ , and let  $\lambda^{(i)}$  and  $\sigma^{(i)}$  be the partitions corresponding to the configuration of white and black points obtained by changing colours of  $q$  and  $q_i$ ,  $i = 1, \dots, k$  (i.e., colour  $q$  black and  $q_i$  white, and leave all other colours unchanged). Then by Theorem 1 we have:

$$s_{\lambda/\mu} \cdot s_{\sigma/\mu} = \sum_{i=1}^k s_{\lambda^{(i)}/\mu} \cdot s_{\sigma^{(i)}/\mu}$$

Figure 6 illustrates this example for

$$\begin{aligned} \lambda &= (16, 15, 15, 13, 13, 11, 11, 10, 10, 9, 7, 5), \\ \sigma &= (14, 14, 12, 12, 11, 11, 11, 9, 8, 7, 7, 5). \end{aligned}$$

From the pictures in Figure 6 we see that  $k = 2$  in this case, with

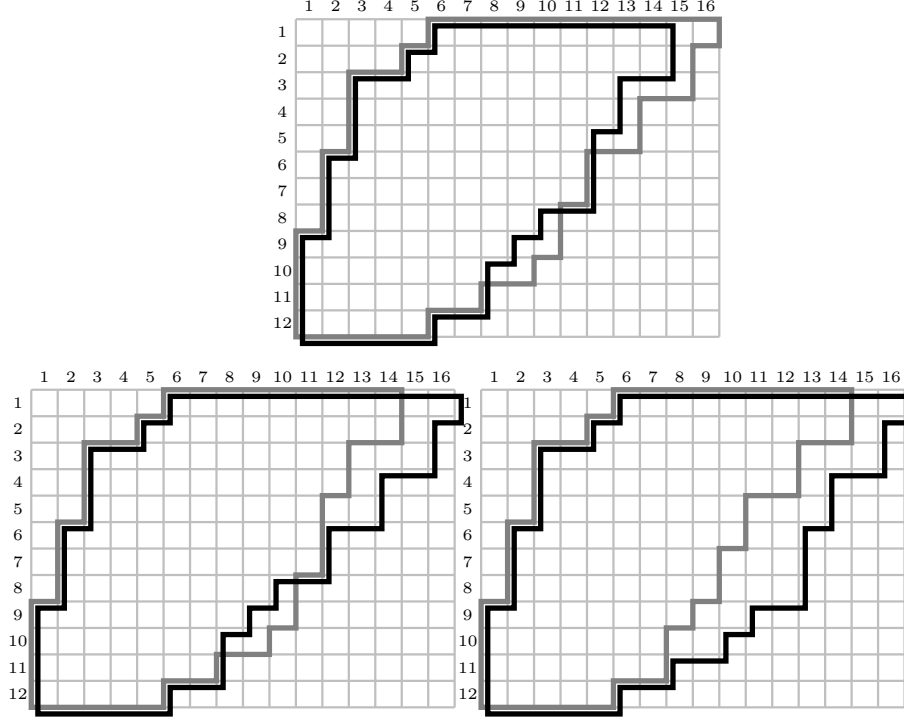
$$\begin{aligned} \lambda^{(1)} &= (14, 14, 12, 12, 11, 11, 11, 10, 10, 9, 7, 5), \\ \sigma^{(1)} &= (16, 15, 15, 13, 13, 11, 11, 9, 8, 7, 7, 5), \end{aligned}$$

(shown in the middle row of Figure 6) and

$$\begin{aligned} \lambda^{(2)} &= (14, 14, 12, 12, 10, 10, 9, 9, 8, 7, 7, 5), \\ \sigma^{(2)} &= (16, 15, 15, 13, 13, 12, 12, 12, 10, 9, 7, 5) \end{aligned}$$

(shown in the lower row of Figure 6). Figure 7 presents the Ferrers diagrams for this example, where we chose  $\mu = \tau = (5, 4, 2, 2, 2, 1, 1, 1)$ .

FIGURE 7. The skew Ferrers boards corresponding to the example in Figure 6 for  $\mu = \tau = (5, 4, 2, 2, 2, 1, 1, 1)$ : The upper picture shows the Ferrers board of  $\lambda/\mu$  (drawn with grey lines) and  $\sigma/\tau$  (drawn with black lines). The lower pictures show the Ferrers boards of  $\lambda^{(i)}/\mu$  and  $\sigma^{(i)}/\tau$ ,  $i = 1, 2$ .



**4.1. The identity of Gurevich, Pyatov and Saponov.** Now consider the special case  $\mu = \tau$ ,  $\lambda_1 > \sigma_1$ ,  $\ell(\lambda) = \ell(\sigma) + 1$ , with shift 0 for all starting and ending points, and where black and white points alternate in their circular orientation. As in Example 1, let  $q = (\lambda_1 - 1, N)$  and choose  $S = \{q\}$ . The possible ending points of the bicoloured path  $b$  ending in  $q$  are

- the black points at level  $N$
- and the leftmost white starting point  $q_0$ .

As our running example we choose the skew shapes  $\lambda/\mu$  and  $\sigma/\tau$  with

$$\begin{aligned}\lambda &= (10, 7, 7, 6, 6, 4, 4, 3, 2, 2), \\ \sigma &= (8, 7, 7, 5, 4, 4, 2, 1, 1), \\ \mu = \tau &= (4, 3, 3, 1).\end{aligned}$$

See the upper picture in Figure 8 for an illustration.

Assume that there are  $k > 1$  black points  $q_1, \dots, q_k$  and denote the shapes corresponding to recolouring  $q$  and  $q_i$ ,  $i = 0, 1, \dots, k$ , by  $\lambda^{(i)}/\mu$  and  $\sigma^{(i)}/\mu$ , respectively. Then by

FIGURE 8. Application of Theorem 1 to the special case  $\mu = \tau$ ,  $\lambda_1 > \sigma_1$ ,  $\ell(\lambda) = \ell(\sigma) + 1$  and shift 0 for all starting and ending points: Consider the configurations that can arise by recolouring the bicoloured path  $b$  ending in  $q = (\lambda_1 - 1, N)$ . The uppermost picture shows the configuration of the starting and ending points of  $\lambda/\mu$  (drawn as white circles) and  $\sigma/\tau$  (drawn as black circles), where  $\mu = \tau = (4, 3, 3, 1)$ . The point  $q = (\lambda_1 - 1, N)$  is marked by a white rectangle.

The three pictures below show the three possible configurations arising by the recolouring of  $b$ ; the other ending point of  $b$  is marked by a white rectangle.

From Theorem 1 we obtain the Schur function identity

$$s_{\lambda/\mu} \cdot s_{\sigma/\tau} = s_{\lambda^{(0)}/\mu} \cdot s_{\sigma^{(0)}/\mu} + s_{\lambda^{(1)}/\mu} \cdot s_{\sigma^{(1)}/\mu} + s_{\lambda^{(2)}/\mu} \cdot s_{\sigma^{(2)}/\mu}.$$

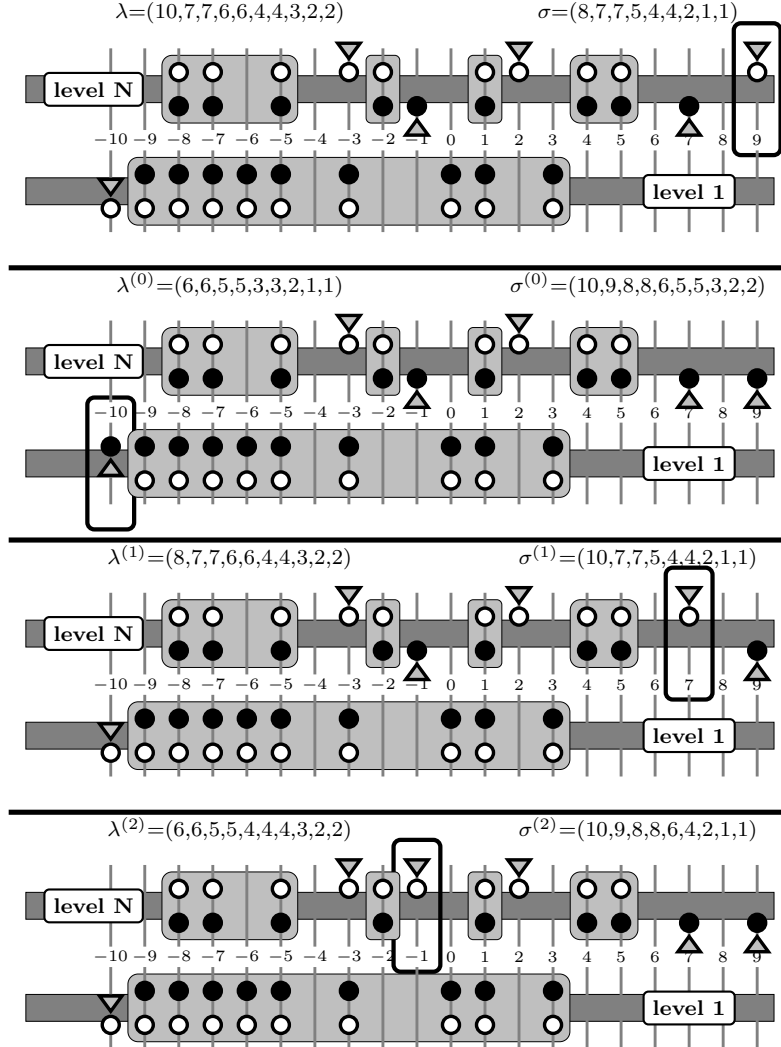
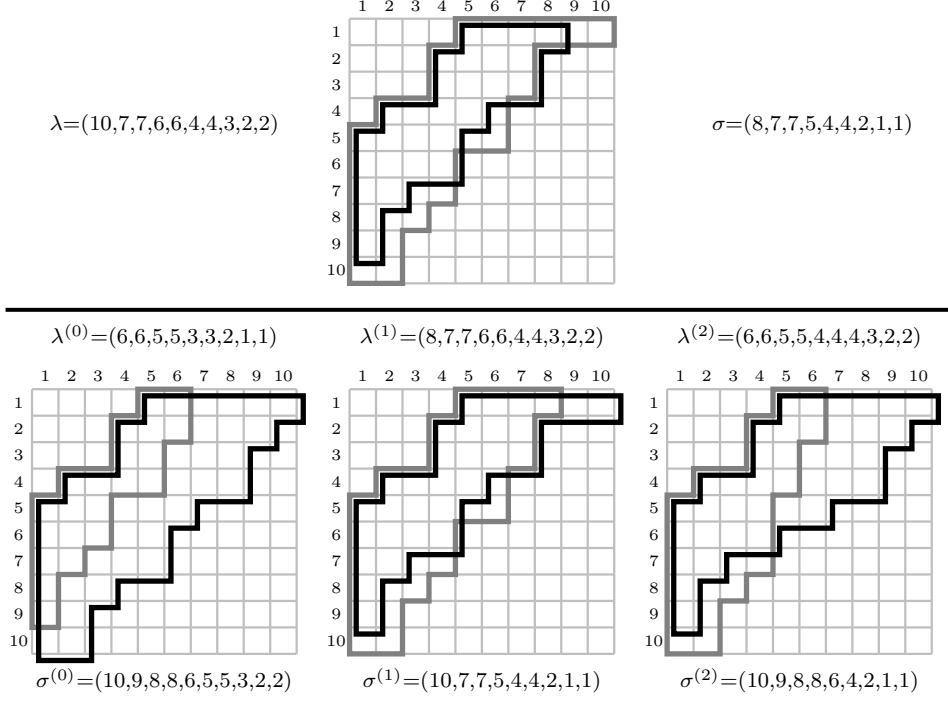


FIGURE 9. The skew Ferrers diagrams corresponding to the example in Figure 8: The upper picture shows the overlay of the Ferrers diagrams for  $\lambda/\mu$  and  $\sigma/\mu$  (without recolouring), and the lower pictures show the overlay of diagrams  $\lambda^{(i)}/\mu$  and  $\sigma^{(i)}/\mu$ ,  $i = 0, 1, 2$ .



Theorem 1 we have:

$$s_{\lambda/\mu} \cdot s_{\sigma/\mu} = s_{\lambda^{(0)}/\mu} \cdot s_{\sigma^{(0)}/\mu} + \sum_{i=1}^k s_{\lambda^{(i)}/\mu} \cdot s_{\sigma^{(i)}/\mu} \quad (8)$$

See the three lower pictures in Figure 8 for an illustration (in this example,  $k = 2$ ).

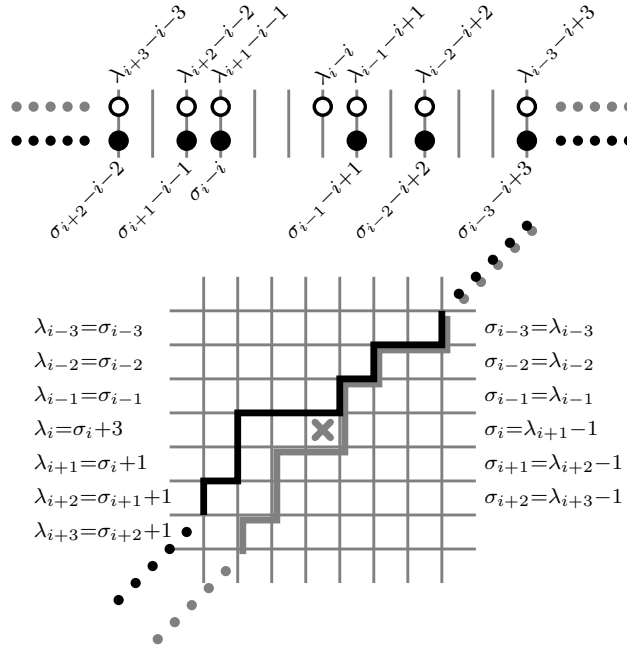
If we choose  $\mu = 0$ , (8) amounts precisely to the identity [4, (3.3)]: We simply have to *translate* our formulation to the language of adding and removing *partial border strips* to Ferrers diagrams, which was used by Gurevich, Pyatov and Saponov [4]. To get a first idea, have a look at Figure 9, which presents the Ferrers diagrams corresponding to the concrete example of Figure 8.

Observe that recolouring starting/ending points may be viewed as a game of insert-ing/removing points in the configuration of starting/ending points corresponding to some partition. Instead of giving a lengthy verbal description, we present in Figure 10 the effect of inserting (read the upper picture upwards, from  $\sigma$  to  $\lambda$ ) or removing (read the upper picture downwards, from  $\lambda$  to  $\sigma$ ) points in a graphical way.

Reading the upper part of Figure 10 *downwards* (i.e., removing the point in position  $\lambda_i - i$ ), the Ferrers diagram of  $\sigma$  is obtained from the Ferrers diagram of  $\lambda$  by a *down-peeling* of a *partial border strip* starting at row  $i$ , or, in the language of [4]:

$$\sigma = \lambda \downarrow^i.$$

FIGURE 10. The operation of inserting/removing points in the configuration of starting/ending points can be translated to the language introduced in [4], i.e., to operations on Ferrers diagrams: In the lower part of the picture, the grey lines correspond to the Ferrers diagram of  $\lambda$ , and the black lines correspond to the Ferrers diagram of  $\sigma$ . Reading the upper part of the picture *downwards* (i.e., removing the point in position  $\lambda_i - i$ ), the Ferrers diagram of  $\sigma$  is obtained from the Ferrers diagram of  $\lambda$  by a *down-peeling* of a *partial border strip* starting at row  $i$ :  $\sigma = \lambda \downarrow^i$ . The partial border strip is the area between the black and grey shapes in rows  $i, i+1, \dots$ : It is clear that such strip begins with the last box in row  $i$  (indicated by a grey "x" in the picture).



The special case of this operation for  $i = 1$  amounts to the removal of the *complete* border strip — in the language of [4]:

$$\lambda \downarrow := \lambda \downarrow^1.$$

Now observe that a pair of partitions  $(\lambda, \sigma)$  fulfilling the preconditions for (8) can be obtained by *constructing* an appropriate  $\sigma$  for a given  $\lambda$ . This is achieved by applying to the configuration of ending points corresponding to  $\lambda$  a sequence of  $k$  removals/insertions of points, followed by removing the right-most ending point and inserting a new left-most starting point, see the upper picture in Figure 8.

Again, we shall illustrate the simple procedure by pictures instead of giving a lengthy verbal description.

The first step of this construction is illustrated in Figure 11: The configuration of points corresponding to the partition  $\lambda = (10, 7, 7, 6, 6, 4, 4, 3, 2, 2)$  considered in Figure 8 is presented in the upper part of the picture. This configuration is changed by adding a

new point at position 7 first (the result of this change is presented in the middle part of the picture) and then by removing the point at position 2 (the result of this change is presented in the lower part of the picture). It is obvious that this amounts to adding a *partial border strip* to the Ferrers diagram of  $\lambda$ , which consists of  $t_1 = 2$  boxes in row  $r_1 = 2$  and spans the  $m_1 = 3$  rows 2, 3 and 4. Stated in the language introduced in [4], the picture in the lower row of Figure 11 shows

$$\lambda +_{(r_1, m_1)}^{t_1}.$$

The next step of this construction is to add a point at position  $-1$  and to remove the point at position  $-3$ . This amounts to adding a partial border strip consisting of  $t_2 = 2$  boxes in row  $r_2 = 6$  and spanning the  $m_2 = 2$  rows 6 and 7. We thus obtain  $\nu = (10, 9, 8, 8, 6, 5, 5, 3, 2, 2)$ , or, in the language of [4]:  $\nu = \lambda +_{(2,3),(6,2)}^{2,1}$ , see the upper picture in Figure 12.

Finally, we remove the rightmost ending point at position 9: This amounts to removing a *complete* border strip from the Ferrers diagram of  $\nu$ , giving the partition  $\sigma = \nu \downarrow = (8, 7, 7, 5, 4, 4, 2, 1, 1)$  of our running example, see the lower picture in Figure 12.

So we see that the Schur function identity stated in Figure 8 can be partially translated as:

$$s_{\lambda/\mu} \cdot s_{\nu \downarrow / \tau} = s_{\lambda \downarrow / \mu} \cdot s_{\nu / \mu} + \cdots$$

To complete this translation, have a look at Figure 13 and note that the partitions  $\lambda^{(1)}$  and  $\lambda^{(2)}$  (drawn with black lines) are obtained by the original partition  $\lambda$  (drawn with grey lines) by removing a partial border strip which starts in the box marked with a small “x” and extends up to the first row. Note that for such *up-peeling* of a border strip starting at row  $i$ , there are  $\lambda_i - \lambda_{i+1}$  possible positions of the starting box: Number them from left to right, then the up-peeling is uniquely determined by the row number  $i$  and the box number  $t$ . In the language of [4], this is denoted by

$$\lambda \uparrow_{(i,t)},$$

i.e., we have  $\lambda^{(1)} = \lambda \uparrow_{(1,2)}$  and  $\lambda^{(2)} = \lambda \uparrow_{(5,1)}$ .

Putting all these observations together, we see that the Schur function identity stated in Figure 8 can be translated as:

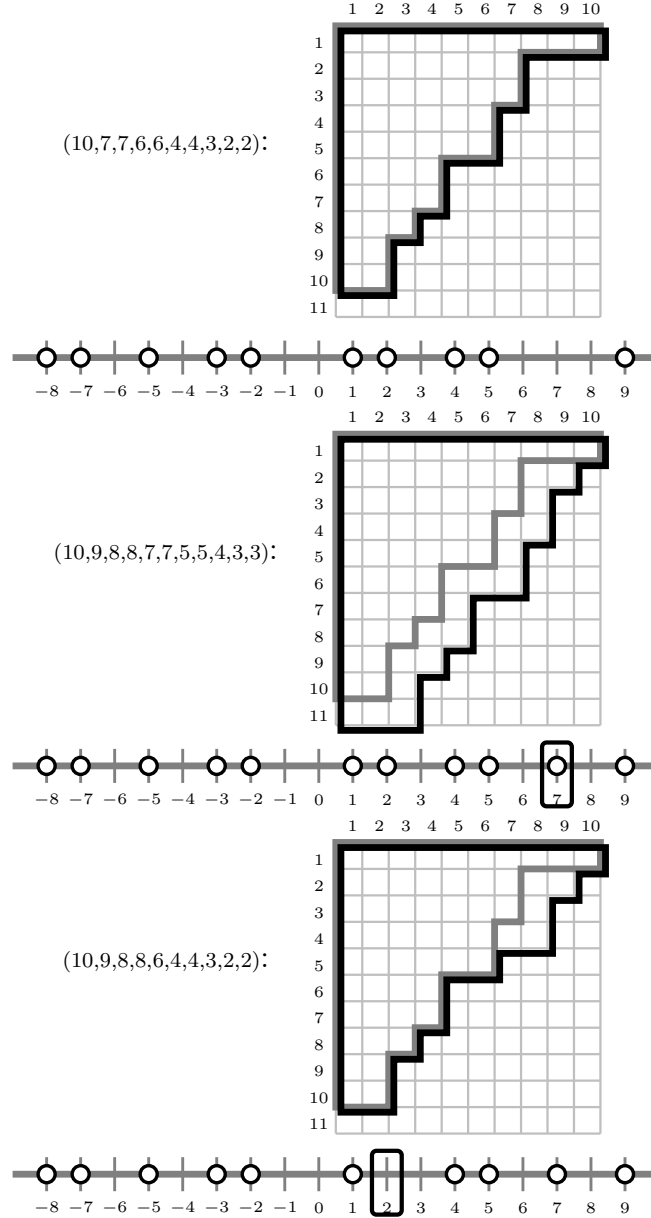
$$s_{\lambda/\mu} \cdot s_{\nu \downarrow / \tau} = s_{\lambda \downarrow / \mu} \cdot s_{\nu / \mu} + s_{\lambda \uparrow_{(1,2)} / \mu} \cdot s_{\nu \downarrow^2 / \mu} + s_{\lambda \uparrow_{(5,1)} / \mu} \cdot s_{\nu \downarrow^6 / \mu}.$$

So it is clear that the special case considered in this section can be stated as follows:

**Corollary 1** (Gurevich, Pyatov and Saponov). *Let  $\lambda = (\lambda_1, \dots, \lambda_r)$  be a partition. Assume that there are  $k$  indices  $2 \leq r_1 < \dots < r_k \leq r$  such that  $\lambda_{r_i} < \lambda_{r_{i-1}}$ ,  $i = 1, \dots, k$ . Choose integers  $t_i$  and  $m_i$  for  $i = 1, \dots, k$  subject to the restrictions*

$$\begin{aligned} 1 &\leq t_i \leq \lambda_{r_{i-1}} - \lambda_{r_i}, \\ 1 &\leq m_i \leq r_{i+1} - r_i. \end{aligned}$$

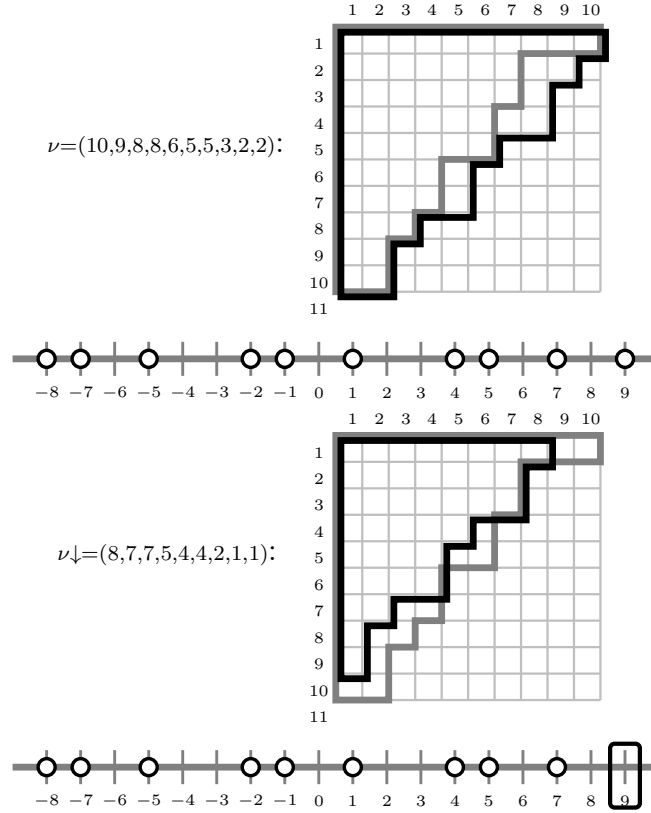
FIGURE 11. Adding some point at position  $i$  and removing a point at position  $j < i$  amounts to adding a *partial border strip*. The pictures show the Ferrers diagram of the original partition  $\lambda$  with grey lines, and the Ferrers diagrams of the partitions obtained by adding/removing points with black lines. The corresponding configuration of ending points is depicted under the Ferrers diagrams.



Then we may construct  $\nu = \lambda \uparrow_{(r_1, m_1) \dots (r_k, m_k)}^{t_1, \dots, t_k}$ , and we have

$$s_\lambda \cdot s_{\nu \downarrow} = s_{\lambda \downarrow} \cdot s_\nu + \sum_{i=1}^k s_{\lambda \uparrow_{(r_i-1, t_i)}} \cdot s_{\nu \downarrow(r_i)}.$$

FIGURE 12. Removing the point corresponding to  $\nu_1$  (marked by a white rectangle in the lower picture) amounts to removing the *complete border strip* spanning rows 1, 2,  $\dots$ ,  $\ell(\nu)$  from the Ferrers board of  $\nu$ , see Figure 10.



## REFERENCES

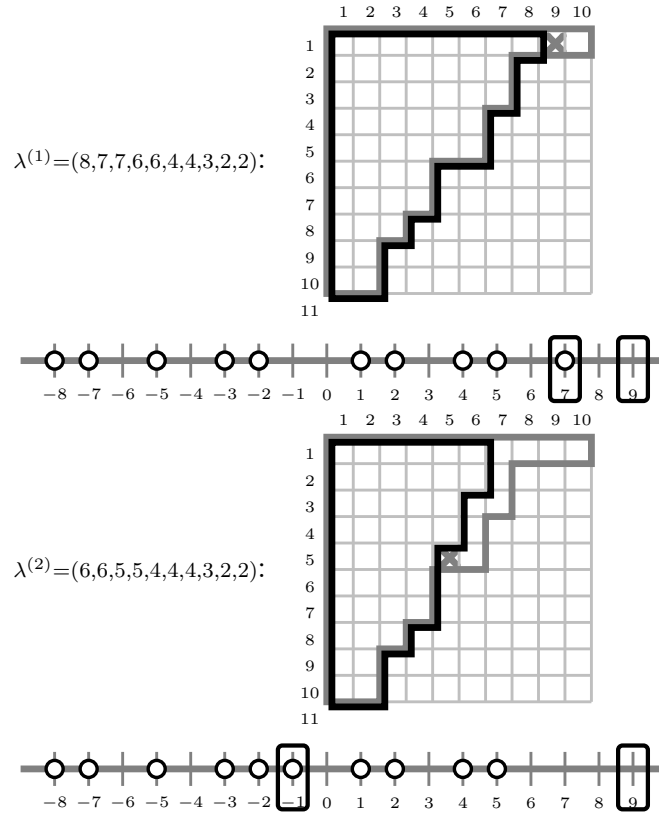
- [1] Markus Fulmek and Michael Kleber. Bijective proofs for Schur function identities which imply Dodgson's condensation formula and Plücker relations. *Electron. J. Combin.*, 8(1):Research Paper 16, 22 pp. (electronic), 2001.
- [2] Ira M. Gessel and Xavier Viennot. Determinants, paths, and plane partitions. preprint, 1998.
- [3] Ian P. Goulden. Quadratic forms of skew Schur functions. *European J. of Combinatorics*, 9:161–168, 1988.
- [4] Dimitri Gurevich, Pavel Pyatov, and Pavel Saponov. Bilinear identities on Schur symmetric functions. arXiv:0907.4292v1 [math.CO].
- [5] Bruce E. Sagan. *The Symmetric Group*. Springer, 2nd edition, 2000.

FAKULTÄT FÜR MATHEMATIK, NORDBERGSTRASSE 15, A-1090 WIEN, AUSTRIA

E-mail address: Markus.Fulmek@Univie.Ac.At

WWW: <http://www.mat.univie.ac.at/~mfulmek>

FIGURE 13. Removing the point corresponding to  $\lambda_1$  and inserting a new point at positions 7 and  $-1$ , respectively (these points are marked by white rectangles in the pictures) yield the partitions  $\lambda^{(1)}$  and  $\lambda^{(2)}$  from Figure 8, respectively. In the language of [4],  $\lambda^{(1)}$  is obtained by the *up-peeling* of a partial border strip starting in row 1 at the second possible box (marked by a grey “x” in the upper picture), and  $\lambda^{(2)}$  is obtained by the up-peeling of a partial border strip starting in row 5 at the first possible box (marked by a grey “x” in the upper picture):  $\lambda^{(1)} = \lambda \uparrow_{(1,2)}$  and  $\lambda^{(2)} = \lambda \uparrow_{(5,1)}$ .



# BIJECTIVE PROOFS FOR SCHUR FUNCTION IDENTITIES WHICH IMPLY DODGSON'S CONDENSATION FORMULA AND PLÜCKER RELATIONS

MARKUS FULMEK  
MICHAEL KLEBER

**ABSTRACT.** We present a “method” for bijective proofs for determinant identities, which is based on translating determinants to Schur functions by the Jacobi–Trudi identity. We illustrate this “method” by generalizing a bijective construction (which was first used by Goulden) to a class of Schur function identities, from which we shall obtain bijective proofs for Dodgson’s condensation formula, Plücker relations and a recent identity of the second author.

## 1. INTRODUCTION

Usually, bijective proofs of determinant identities involve the following steps (cf., e.g. [19, Chapter 4] or [23, 24]):

- Expansion of the determinant as sum over the symmetric group,
- Interpretation of this sum as the generating function of some set of combinatorial objects which are equipped with some signed weight,
- Construction of an explicit weight– and sign–preserving bijection between the respective combinatorial objects, maybe supported by the construction of a sign–reversing involution for certain objects.

Here, we will present another “method” of bijective proofs for determinant identities, which involves the following steps:

- First, we replace the entries  $a_{i,j}$  of the determinants by  $h_{\lambda_i - i + j}$  (where  $h_m$  denotes the  $m$ –th complete homogeneous function),
- Second, by the Jacobi–Trudi identity we transform the original determinant identity into an equivalent identity for Schur functions,

- Third, we obtain a bijective proof for this equivalent identity by using the interpretation of Schur functions in terms of non-intersecting lattice paths. (In this paper, we shall achieve this with a construction which was used for the proof of a Schur function identity [3, Theorem 1.1] conjectured by Ciucu.)

We show how this method applies naturally to provide elegant bijective proofs of Dodgson’s Condensation Rule [2] and the Plücker relations.

The bijective construction we use here was (to the best of our knowledge) first used by I. Goulden [7]. (The first author is grateful to A. Hamel [8] for drawing his attention to Goulden’s work.) Goulden’s exposition, however, left open a small gap, which we shall close here.

The paper is organized as follows: In Section 2, we present the theorems we want to prove, and explain Steps 1 and 2 of our above “method” in greater detail. In Section 3, we briefly recall the combinatorial definition of Schur functions and the Gessel–Viennot–approach. In Section 4, we explain the bijective construction employed in Step 3 of our “method” by using the proof of a Theorem from Section 2 as an illustrating example. There, we shall also close the small gap in Goulden’s work. In Section 5, we “extract” the general structure underlying the bijection: As it turns out, this is just a simple graph-theoretic statement. From this we may easily derive a general “class” of Schur function identities which follow from these considerations. In order to show that these quite general identities specialize to something useful, we shall deduce the Plücker relations, using again our “method”. In Section 7, we turn to a theorem [11, Theorem 3.2] recently proved by the second author by using Plücker relations: We explain how this theorem fits into our construction and give a bijective proof using inclusion–exclusion.

## 2. EXPOSITION OF IDENTITIES AND PROOFS

The origin of this paper was the attempt to give a bijective proof of the following identity for Schur functions, which arose in work of Kirillov [10]:

**Theorem 1.** *Let  $c, r$  be positive integers; denote by  $[c^r]$  the partition consisting of  $r$  rows with constant length  $c$ . Then we have the following identity for Schur functions:*

$$(s_{[c^r]})^2 = s_{[c^{r-1}]} \cdot s_{[c^{r+1}]} + s_{[(c-1)^r]} \cdot s_{[(c+1)^r]}. \quad (1)$$

(See [18, 7.10], [5], [13] or [16] for background information on Schur functions; in order to keep our exposition self-contained, a combinatorial definition is given in Section 4.)

The identity (1) was recently considered by the second author [11, Theorem 4.2], who also gave a bijective proof, and generalized it considerably [11, Theorem 3.2].

The construction we use here does in fact prove a more general statement:

**Theorem 2.** *Let  $(\lambda_1, \lambda_2, \dots, \lambda_{r+1})$  be a partition, where  $r > 0$  is some integer. Then we have the following identity for Schur functions:*

$$\begin{aligned} s_{(\lambda_1, \dots, \lambda_r)} \cdot s_{(\lambda_2, \dots, \lambda_{r+1})} \\ = s_{(\lambda_2, \dots, \lambda_r)} \cdot s_{(\lambda_1, \dots, \lambda_{r+1})} + s_{(\lambda_2-1, \dots, \lambda_{r+1}-1)} \cdot s_{(\lambda_1+1, \dots, \lambda_{r+1})}. \end{aligned} \quad (2)$$

Clearly, Theorem 1 is a direct consequence of Theorem 2: Simply set  $\lambda_1 = \dots = \lambda_{r+1} = c$ .

Theorem 2, however, is in fact equivalent to Dodgson's condensation formula [2], which is also known as Desnanot–Jacobi's adjoint matrix theorem (see [1, Theorem 3.12]: According to [1], Lagrange discovered this theorem for  $n = 3$ , Desnanot proved it for  $n \leq 6$  and Jacobi published the general theorem [9], see also [14, vol. I, pp. 142]):

**Theorem 3.** *Let  $A$  be an arbitrary  $(r+1) \times (r+1)$ -determinant. Denote by  $A_{\{r_1, r_2\}, \{c_1, c_2\}}$  the minor consisting of rows  $r_1, r_1+1, \dots, r_2$  and columns  $c_1, c_1+1, \dots, c_2$  of  $A$ . Then we have the following identity:*

$$\begin{aligned} A_{\{1, r+1\}, \{1, r+1\}} A_{\{2, r\}, \{2, r\}} \\ = A_{\{1, r\}, \{1, r\}} A_{\{2, r+1\}, \{2, r+1\}} - A_{\{2, r+1\}, \{1, r\}} A_{\{1, r\}, \{2, r+1\}}. \end{aligned} \quad (3)$$

The transition from Theorem 3 to Theorem 2 is established by the Jacobi–Trudi identity (see [13, I, (3.4)]), which states that for any partition  $\lambda = (\lambda_1, \dots, \lambda_r)$  of length  $r$  we have

$$s_\lambda = \det(h_{\lambda_i - i + j})_{i,j=1}^r, \quad (4)$$

where  $h_m$  denotes the  $m$ -th complete homogeneous symmetric function: Setting  $A_{i,j} := h_{\lambda_i - i + j}$  for  $1 \leq i, j \leq r+1$  in Theorem 3 and using identity (4) immediately yields (2).

That the seemingly weaker statement of Theorem 2 does in fact imply Theorem 3 is due to the following observation: Choose  $\lambda$  so that the numbers  $\lambda_i - i + j$  are all distinct for  $1 \leq i, j \leq (r+1)$  (e.g.,  $\lambda = ((r+1)r, r^2, (r-1)r, \dots, r)$  would suffice) and rewrite (2) as a determinantal expression according to the Jacobi–Trudi identity (4). This yields a special case of identity (3) with  $A_{i,j} := h_{\lambda_i - i + j}$  as above.

Now recall that the complete homogeneous symmetric functions are algebraically independent (see, e.g., [21]), whence the identity (3) is true for generic  $A_{i,j}$ . For later use, we record this simple observation in a more general fashion:

**Observation 4.** *Let  $\mathcal{I}$  be an identity involving determinants of homogeneous symmetric functions  $h_n$ , where  $n$  is some nonnegative integer. Then  $\mathcal{I}$  is, in fact, equivalent to a general determinant identity which is obtained from  $\mathcal{I}$  by considering each  $h_n$  as a formal variable.*

So far, the promised proof (to be given in Section 4) of Theorem 2 would give a new bijective proof of Dodgson’s Determinant–Evaluation Rule (a beautiful bijective proof was also given by Zeilberger [23]). But we can do a little better: Our bijective construction does, in fact, apply to a quite general “class of Schur function identities”, a special case of which implies the Plücker relations (also known as Grassmann–Plücker syzygies), see, e.g., [21], or [22, Chapter 3, Section 9, formula II]:

**Theorem 5** (Plücker relations). *Consider an arbitrary  $2n \times n$ -matrix with row indices  $1, 2, \dots, 2n$ . Denote the  $n \times n$ -minor of this matrix consisting of rows  $i_1, \dots, i_n$  by  $[i_1, \dots, i_n]$ .*

*Consider some fixed list of integers  $1 \leq r_1 < r_2 < \dots < r_k \leq n$ ,  $0 \leq k \leq n$ . Then we have:*

$$[1, 2, \dots, n] \cdot [n+1, n+2, \dots, 2n] = \sum_{n+1 \leq s_1 < s_2 < \dots < s_k \leq 2n} [1, \dots, s_1, \dots, s_k, \dots, n] \cdot [n+1, \dots, r_1, \dots, r_k, \dots, 2n], \quad (5)$$

where the notation of the summands means that rows  $r_i$  were exchanged with rows  $s_i$ , respectively.

This is achieved by observing that (5) can be specialized to a Schur function identity of the form

$$s_\lambda s_\mu = \sum_{\lambda', \mu'} s_{\lambda'} s_{\mu'},$$

where  $\lambda$  and  $\mu$  are partitions with the same number  $n$  of parts, and where the sum is over certain pairs  $\lambda', \mu'$  derived from  $\lambda, \mu$  (to be described later). This Schur function identity belongs to the “class of identities” which follow from the bijective construction. By applying Observation 4 with suitable  $\lambda$  and  $\mu$ , we may deduce (5).

**Remark 6.** *Summing equation (5) over all possible choices of subsets  $\{r_1, \dots, r_k\}$  yields the determinant identity behind Ciucu’s Schur*

function identity [3, Theorem 1.1]

$$\sum_{A \subset T: |A|=k} s_{\lambda(A)} s_{\lambda(T-A)} = 2^k s_{\lambda(t_2, \dots, t_{2k})} s_{\lambda(t_1, \dots, t_{2k-1})}, \quad (6)$$

where  $T = \{t_1 < \dots < t_{2k}\}$  is some set of positive integers and  $\lambda(\{t_{i_1} < \dots < t_{i_r}\})$  denotes the partition with parts  $t_{i_r} - r + 1 \geq \dots \geq t_{i_2} - 1 \geq t_{i_1}$ .

**Remark 7.** The Plücker relations (5) appear in a slightly different notation as Theorem 2 in [15], together with another elegant proof.

Moreover, the bijective method yields a proof of the second author's theorem [11, Theorem 3.2]: Since this theorem is rather complicated to state, we defer it to Section 7.

### 3. COMBINATORIAL BACKGROUND AND DEFINITIONS

As usual, an  $r$ -tuple  $\lambda = (\lambda_1, \lambda_2, \dots, \lambda_r)$  with  $\lambda_1 \geq \lambda_2 \geq \dots \geq \lambda_r \geq 0$  is called a *partition of length  $r$* . The *Ferrers board*  $F(\lambda)$  of  $\lambda$  is an array of cells with  $r$  left-justified rows and  $\lambda_i$  cells in row  $i$ .

An  $N$ -semistandard Young tableau of shape  $\lambda$  is a filling of the cells of  $F(\lambda)$  with integers from the set  $\{1, 2, \dots, N\}$ , such that the numbers filled into the cells weakly increase in rows and strictly increase in columns (see the right picture of Figure 1 for an illustration).

Schur functions, which are irreducible general linear characters, can be combinatorially defined by means of  $N$ -semistandard Young tableaux (see [13, I, (5.12)], [16, Def. 4.4.1], [17, Def. 5.1]):

$$s_{\lambda}(x_1, x_2, x_3, \dots, x_N) = \sum_{\mathbf{T}} w(\mathbf{T}),$$

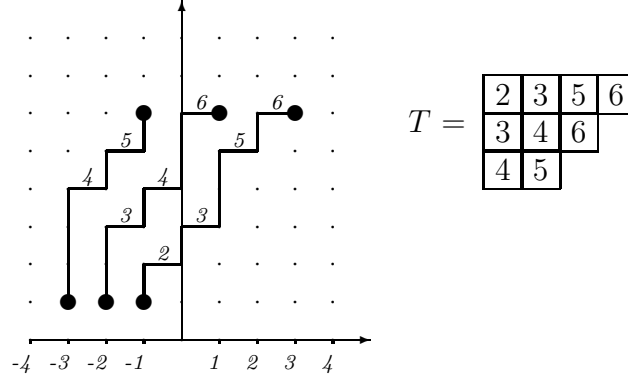
where the sum is over all  $N$ -semistandard Young tableaux  $\mathbf{T}$  of shape  $\lambda$ . Let  $m(\mathbf{T}, k)$  be the number of entries  $k$  in the tableau  $\mathbf{T}$ . The weight  $w(\mathbf{T})$  of  $\mathbf{T}$  is defined as follows:

$$w(\mathbf{T}) = \prod_{k=1}^N x_k^{m(\mathbf{T}, k)}.$$

The Gessel-Viennot interpretation [6] of semistandard Young tableaux of shape  $\lambda$  as nonintersecting lattice paths (see the left picture of Figure 1 for an illustration) allows an equivalent definition of Schur functions:

$$s_{\lambda}(x_1, x_2, x_3, \dots, x_N) = \sum_{\mathbf{P}} w(\mathbf{P}),$$

FIGURE 1. Illustration of a 6-semistandard Young tableau and its associated lattice paths for  $\lambda = (4, 3, 2)$ .



where the sum is over all  $r$ -tuples  $\mathbf{P} = (P_1, P_2, \dots, P_r)$  of lattice paths (in the integer lattice, i.e., the directed graph with vertices  $\mathbb{Z} \times \mathbb{Z}$  and arcs from  $(j, k)$  to  $(j + 1, k)$  and from  $(j, k)$  to  $(j, k + 1)$  for all  $j, k$ ), where  $P_i$  starts at  $(-i, 1)$  and ends at  $(\lambda_i - i, N)$ , and where no two paths  $P_i$  and  $P_j$  have a lattice point in common (such an  $r$ -tuple is called nonintersecting).

The weight  $w(\mathbf{P})$  of an  $r$ -tuple  $\mathbf{P} = (P_1, P_2, \dots, P_r)$  of paths is defined by:

$$w(\mathbf{P}) = \prod_{i=1}^r w(P_i).$$

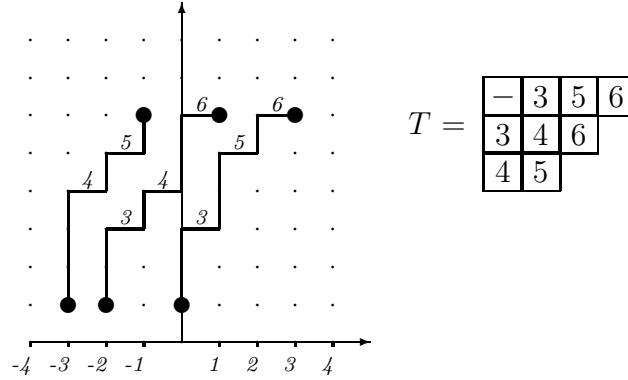
The weight  $w(P)$  of a single path  $P$  is defined as follows: Let  $n(P, k)$  be the number of horizontal steps at height  $k$  (i.e., directed arcs from some  $(j, k)$  to  $(j + 1, k)$ ) that belong to path  $P$ , then we define

$$w(P) = \prod_{k=1}^N x_k^{n(P, k)}.$$

That these definitions are in fact equivalent is due to a weight-preserving bijection between tableaux and nonintersecting lattice paths. The Gessel–Viennot method [6] builds on the lattice path definition to give a bijective proof of the Jacobi–Trudi identity (4) (see, e.g., [16, ch. 4], [20] or [4]).

Next, we give a combinatorial definition for *skew* Schur functions: Let  $\lambda = (\lambda_1, \dots, \lambda_r)$  and  $\mu = (\mu_1, \dots, \mu_r)$  be partitions with  $\mu_i \leq \lambda_i$  for  $1 \leq i \leq r$ ; here, we allow  $\mu_i = 0$ .

FIGURE 2. Illustration of a 6-semistandard skew Young tableau and its associated lattice paths for  $\lambda = (4, 3, 2)$  and  $\mu = (1, 0, 0)$ .



The *skew Ferrers board*  $F(\lambda/\mu)$  of  $(\lambda, \mu)$  is an array of cells with  $r$  left-justified rows and  $\lambda_i - \mu_i$  cells in row  $i$ , where the first  $\mu_i$  cells in row  $i$  are missing.

An  $N$ -semistandard skew Young tableau of shape  $\lambda/\mu$  is a filling of the cells of  $F(\lambda/\mu)$  with integers from the set  $\{1, 2, \dots, N\}$ , such that the numbers filled into the cells weakly increase in rows and strictly increase in columns (see the right picture of Figure 2 for an illustration).

Then we have the following definition for skew Schur functions:

$$s_{\lambda/\mu}(x_1, x_2, x_3, \dots, x_N) = \sum_{\mathbf{T}} w(\mathbf{T}),$$

where the sum is over all  $N$ -semistandard skew Young tableaux  $\mathbf{T}$  of shape  $\lambda/\mu$ , where the weight  $w(\mathbf{T})$  of  $\mathbf{T}$  is defined as before.

Equivalently, we may define:

$$s_{\lambda/\mu}(x_1, x_2, x_3, \dots, x_N) = \sum_{\mathbf{P}} w(\mathbf{P}),$$

where the sum is over all  $r$ -tuples  $\mathbf{P} = (P_1, P_2, \dots, P_r)$  of nonintersecting lattice paths, where  $P_i$  starts at  $(\mu_i - i, 1)$  and ends at  $(\lambda_i - i, N)$  (see the left picture of Figure 2 for an illustration), and where the weight  $w(\mathbf{P})$  of such an  $r$ -tuple  $\mathbf{P}$  is defined as before.

#### 4. BIJECTIVE PROOF OF THEOREM 2

*Proof.* Let us start with a combinatorial description for the objects involved in (2): By the Gessel–Viennot interpretation of Schur functions

as generating functions of nonintersecting lattice paths, we may view the left-hand side of the equation as the weight of all *pairs*  $(\mathbf{P}^g, \mathbf{P}^b)$ , where  $\mathbf{P}^g$  and  $\mathbf{P}^b$  are  $r$ -tuples of nonintersecting lattice paths. The paths of  $\mathbf{P}^g$  are coloured green, the paths of  $\mathbf{P}^b$  are coloured blue. The  $i$ -th green path  $P_i^g$  starts at  $(-i, 1)$  and ends in  $(\lambda_i - i, N)$ . The  $i$ -th blue path  $P_i^b$  starts at  $(-i - 1, 1)$  and ends in  $(\lambda_{i+1} - i - 1, N)$ . For an illustration, see the upper left pictures in Figures 3 and 4, where green paths are drawn with full lines and blue paths are drawn with dotted lines.

For the right-hand side of (2), we use the same interpretation. We may view the first term as the weight of all *pairs*  $(\mathbf{A}^g, \mathbf{A}^b)$ , where  $\mathbf{A}^g$  is an  $(r - 1)$ -tuple of nonintersecting lattice paths and  $\mathbf{A}^b$  is an  $(r + 1)$ -tuple of nonintersecting lattice paths. The paths of  $\mathbf{A}^g$  are coloured green, the paths of  $\mathbf{A}^b$  are coloured blue. The  $i$ -th green path  $A_i^g$  starts at  $(-i - 1, 1)$  and ends in  $(\lambda_{i+1} - i - 1, N)$ . The  $i$ -th blue path  $A_i^b$  starts at  $(-i, 1)$  and ends in  $(\lambda_i - i, N)$ . For an illustration, see the upper right picture in Figure 3.

In the same way, we may view the second term as the weight of all *pairs*  $(\mathbf{B}^g, \mathbf{B}^b)$ , where  $\mathbf{B}^g$  and  $\mathbf{B}^b$  are  $r$ -tuples of nonintersecting lattice paths. The paths of  $\mathbf{B}^g$  are coloured green, the paths of  $\mathbf{B}^b$  are coloured blue. The  $i$ -th green path  $B_i^g$  starts at  $(-i, 1)$  and ends in  $(\lambda_{i+1} - i - 1, N)$ . The  $i$ -th blue path  $B_i^b$  starts at  $(-i - 1, 1)$  and ends in  $(\lambda_i - i, N)$ . For an illustration, see the upper right picture in Figure 4.

In any case, the weight of some pair of paths  $(\mathbf{P}, \mathbf{Q})$  is defined as follows:

$$w(\mathbf{P}, \mathbf{Q}) := w(\mathbf{P}) \cdot w(\mathbf{Q}).$$

What we want to do is to give a weight-preserving bijection between the objects on the left side and on the right side:

$$\{(\mathbf{P}^g, \mathbf{P}^b)\} \leftrightarrow (\{(\mathbf{A}^g, \mathbf{A}^b)\} \cup \{(\mathbf{B}^g, \mathbf{B}^b)\}). \quad (7)$$

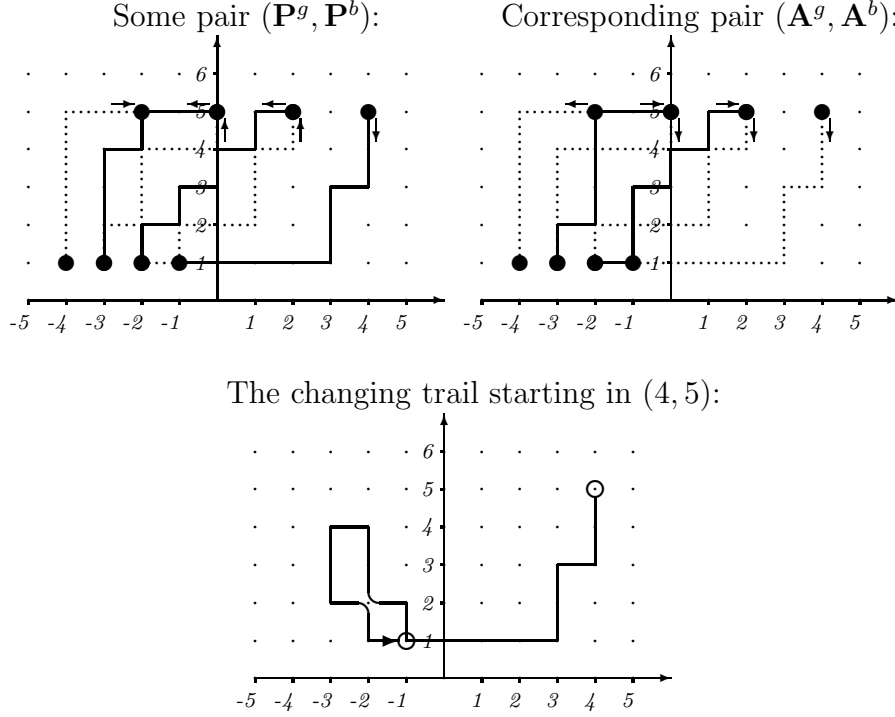
Clearly, such a bijection would establish (2).

The basic idea is very simple and was already used in [7] and in [3]: Since it will be reused later, we state it here quite generally:

**Definition 8.** Let  $\mathbf{P}^1, \mathbf{P}^2$  be two arbitrary families of nonintersecting lattice paths. The paths  $P_i^1$  of the first family are coloured with colour blue, the paths  $P_j^2$  of the second family are coloured with colour green.

Let  $G(\mathbf{P}^1, \mathbf{P}^2)$  be the “two-coloured” graph made up by  $\mathbf{P}^1$  and  $\mathbf{P}^2$  in the obvious sense. Observe that there are the two possible orientations for any edge in that graph: When traversing some path, we may either

FIGURE 3. Illustration of the construction in the proof,  
case A:  $r = 3$ ,  $(\lambda_1, \lambda_2, \lambda_3, \lambda_4) = (5, 4, 3, 2)$ .



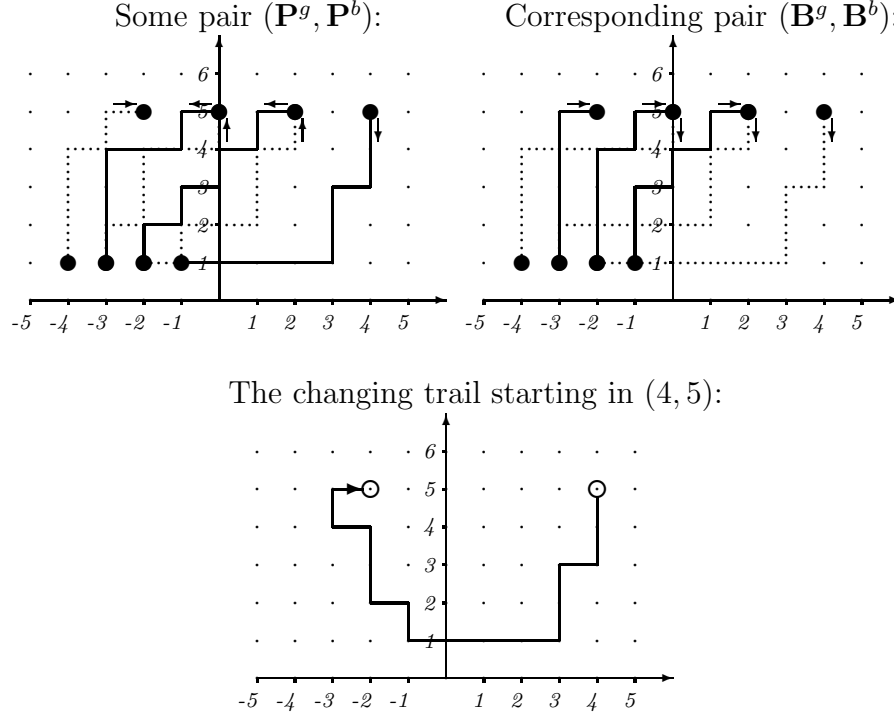
move “right-upwards” (this is the “original” orientation of the paths) or “left-downwards”.

A changing trail is a trail in  $G(\mathbf{P}^1, \mathbf{P}^2)$  with the following properties:

- Subsequent edges of the same colour are traversed in the same orientation, subsequent edges of the opposite colour are traversed in the opposite orientation.
- At every intersection of green and blue paths, colour and orientation are changed if this is possible (i.e., if there is an adjacent edge of opposite colour and opposite orientation); otherwise the trail must stop there.
- The trail is maximal in the sense that it cannot be extended by adjoining edges (in a way which is consistent with the above conditions) at its start or end.

Note that for every edge  $e$ , there is a unique changing trail which contains  $e$ : E.g., consider some blue edge which is right- or upwards-directed and enters vertex  $v$ . If there is an intersection at  $v$ , and if there is a green edge leaving  $v$  (in opposite direction left or downwards), then

FIGURE 4. Illustration of the construction in the proof,  
case B:  $r = 3$ ,  $(\lambda_1, \lambda_2, \lambda_3, \lambda_4) = (5, 4, 3, 2)$ .



the trail must continue with this edge; otherwise it must stop at  $v$ . If there is no intersection at  $v$ , and if there is a blue edge leaving  $v$  (in the same direction right or upwards), then the trail must continue with this edge; otherwise it must stop at  $v$ .

Note that a changing trail is either “path-like”, i.e., has obvious starting point and end point (clearly, these must be the end points or starting points of some path from either  $\mathbf{P}^1$  or  $\mathbf{P}^2$ ), or it is “cycle-like”, i.e., is a closed trail.

Let us return from general definitions to our concrete case: Starting with an object  $(\mathbf{P}^g, \mathbf{P}^b)$  from the left-hand side of (7), we interpret this pair of lattice paths as a graph  $G(\mathbf{P}^g, \mathbf{P}^b)$  with green and blue edges. (See the upper left pictures in Figures 3 and 4.)

Next, we determine the changing trail which starts at the rightmost endpoint  $(\lambda_1 - 1, N)$ : Follow the green edges downward or to the left; at every intersection, change colour and orientation, if this is possible; otherwise stop there. Clearly, this changing trail is “path-like”. (See Figures 3 and 4 for an illustration: There, the orientation of edges

is indicated by small arrows in the upper pictures; the lower pictures show the corresponding changing trails.)

Now we change colours green to blue and vice versa along this changing trail: It is easy to see that this recolouring yields nonintersecting tuples of green and blue lattice paths.

Note that there are exactly two possible cases:

**Case A:** The changing trail stops at the rightmost starting point,  $(-1, 1)$ , of the lattice paths. In this case, from the recolouring procedure we obtain an object  $(\mathbf{A}^g, \mathbf{A}^b)$ ; see the upper right picture in Figure 3.

**Case B:** The changing trail stops at the leftmost endpoint,  $(\lambda_{r+1} - r - 1, N)$ , of the lattice paths. In this case, from the recolouring procedure we obtain an object  $(\mathbf{B}^g, \mathbf{B}^b)$ ; see the upper right picture in Figure 4.

It is clear that altogether this gives a mapping of the set of all objects  $(\mathbf{P}^g, \mathbf{P}^b)$  into the union of the two sets of all objects  $(\mathbf{A}^g, \mathbf{A}^b)$  and  $(\mathbf{B}^g, \mathbf{B}^b)$ , respectively. Of course, this mapping is weight-preserving. It is also injective since the above construction is reversed by simply repeating it, i.e., determine the changing trail starting at the rightmost endpoint  $(\lambda_1 - 1, N)$  (this trail is exactly the same as before, only the colours are exchanged) and change colours. For an illustration, read Figures 3 and 4 from right to left.

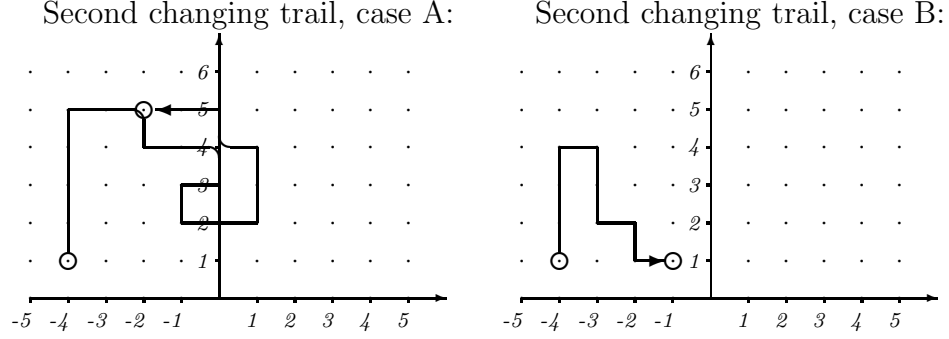
So what is left to prove is surjectivity: To this end, it suffices to prove that if we apply our (injective) recolouring construction to an *arbitrary* object  $(\mathbf{A}^g, \mathbf{A}^b)$  or  $(\mathbf{B}^g, \mathbf{B}^b)$ , we do *always* get an object  $(\mathbf{P}^g, \mathbf{P}^b)$ ; i.e., two  $r$ -tuples of nonintersecting lattice paths, coloured green and blue, and with the appropriate starting points and endpoints.

We *do* have something to prove: Note that in both cases, A (see Figure 3) and B (see Figure 4), there is *prima vista* a second possible endpoint for the changing trail, namely the leftmost starting point,  $(-r - 1, 1)$ , of the lattice paths, where the leftmost blue path starts. If this endpoint could actually be reached, then the resulting object would clearly not be of type  $(\mathbf{P}^g, \mathbf{P}^b)$ . So we have to show that this is impossible. (Goulden left out this indispensable step in [7, Theorem 2.2], but we shall close this small gap immediately.)

**Observation 9.** *The following properties of changing trails are immediate:*

- *If some edge of a changing trail is used by paths of both colours green and blue, then it is necessarily traversed in both orientations and thus forms a changing trail (which is “cycle-like”) by itself.*

FIGURE 5. Illustration of the second changing trails for cases A and B.



- *Two changing trails may well touch each other (i.e., have some vertex in common), but can never cross.*

Now observe that in Case A, there is also a second possible starting point of a “path-like” changing trail, namely the left-most endpoint  $(\lambda_{r+1} - r - 1, N)$  of the lattice paths (see the left picture in Figure 5). Likewise, in Case B, there is a second possible starting point of a “path-like” changing trail, namely the rightmost starting point  $(-1, 1)$  of the lattice paths (see the right picture in Figure 5).

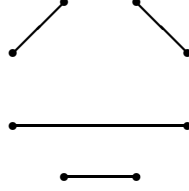
In both cases, if the changing trail starting in  $(\lambda_1 - 1, N)$  would reach the leftmost starting point  $(-r - 1, 1)$  of the lattice paths, it clearly would *cross* this other “path-like” changing trail; a contradiction to Observation 9. (The pictures in Figure 5 shows these other changing trails for the examples in Figures 3 and 4, respectively.)

This finishes the proof.  $\square$

## 5. THE BIJECTIVE CONSTRUCTION, GENERALIZED

It is immediately obvious that the bijective construction used in the proof of Theorem 2 is not at all restricted to the special situation of Theorem 2: We can *always* consider the product of two (arbitrary) skew Schur functions as generating functions of certain “two-coloured graphs” derived from the lattice path interpretation, as above. Determining the changing trails which start in some fixed set of starting points and recolouring their edges will *always* yield an injective (and, clearly, weight-preserving) mapping: The only issue which needs extra care is surjectivity.

FIGURE 6. Illustration of a *perfect* noncrossing matching in  $K_8$ .



In the proof of Theorem 2 we saw that the argument showing surjectivity boils down to a very simple graph-theoretic reasoning. We shall recast this simple reasoning into a general statement:

**Observation 10.** *Consider the complete graph  $K_{2n}$  with  $2n$  vertices, numbered  $1, 2, \dots, 2n$ , and represent its vertices as points on the unit circle (i.e., vertex number  $m$  is represented as  $e^{2m\pi\sqrt{-1}}$ ); represent the edges as straight lines connecting the corresponding vertices. Call a matching in this graph noncrossing if no two of its edges cross each other in this geometric representation (see Figure 6 for an illustration). Then we have:*

*Any edge which belongs to a perfect noncrossing matching must connect an odd-numbered vertex to an even-numbered vertex.*

**Remark 11.** *Note that the number of perfect noncrossing matchings in  $K_{2n}$  is the Catalan number  $C_n$  (see [18, p. 222]).*

**Remark 12.** *Note that the argument proving surjectivity in Theorem 2 amounts to the fact that the two possible “path-like” changing trails connecting the four possible starting points and end points  $(\lambda_1 - 1, N)$ ,  $(\lambda_{r+1} - r - 1, N)$ ,  $(-r - 1, 1)$  and  $(-1, 1)$  must correspond to a noncrossing perfect matching of the complete graph  $K_4$ .*

We shall derive a general statement for skew Schur functions:

Let  $\lambda = (\lambda_1, \dots, \lambda_r)$  and  $\mu = (\mu_1, \dots, \mu_r)$  be partitions with  $0 \leq \mu_i \leq \lambda_i$  for  $1 \leq i \leq r$ ; let  $\sigma = (\sigma_1, \dots, \sigma_r)$  and  $\tau = (\tau_1, \dots, \tau_r)$  be partitions with  $0 \leq \tau_i \leq \sigma_i$  for  $1 \leq i \leq r$ .

**Remark 13.** *We intentionally allow parts of length 0 in the partitions  $\lambda$  and  $\sigma$ : This is equivalent to allowing them to have different numbers of parts.*

Interpret  $s_{\lambda/\mu}$  as the generating function of the family of nonintersecting lattice paths  $(P_1^b, \dots, P_r^b)$ , where  $P_i^b$  starts at  $(\mu_i - i, 1)$  and ends at  $(\lambda_i - i, N)$ . Colour the corresponding lattice paths blue.

Interpret  $s_{\sigma/\tau}$  as the generating function of the family of nonintersecting lattice paths  $(P_1^g, \dots, P_r^g)$ , where  $P_i^g$  starts at  $(\tau_i + t - i, 1)$  and ends at  $(\sigma_i + t - i, N)$ . Colour the corresponding lattice paths green. Here,  $t$  is an arbitrary but fixed integer which indicates the horizontal offset of the green paths with respect to the blue paths.

Consider the sequence of possible starting points of “path-like” changing trails of the corresponding two-coloured graph, in the sense of Section 4, where the end-points of the lattice paths appear in order from right to left in this sequence, followed by the starting points of the lattice paths in order from left to right. Note that the number of such points is even,  $2k$ , say. More precisely, consider  $(x_1, N), \dots, (x_l, N)$ , followed by  $(x_{l+1}, 1), \dots, (x_{2k}, 1)$ , where

$$\begin{aligned} \{x_1, \dots, x_l\} = \{i : \lambda_i - i \neq \sigma_j + t - j \text{ for } 1 \leq j \leq r\} \cup \\ \{j : \sigma_j + t - j \neq \lambda_i - i \text{ for } 1 \leq i \leq r\}, \end{aligned}$$

$x_1 > x_2 > \dots > x_l$ , and where

$$\begin{aligned} \{x_{l+1}, \dots, x_{2k}\} = \{i : \mu_i - i \neq \tau_j + t - j \text{ for } 1 \leq j \leq r\} \cup \\ \{j : \tau_j + t - j \neq \mu_i - i \text{ for } 1 \leq i \leq r\}, \end{aligned}$$

$x_{l+1} < \dots < x_{2k}$ .

Denote this sequence of points  $(x_i, \cdot)$  by  $(Q_i)$ ,  $1 \leq i \leq 2k$ . For  $1 \leq i \leq l$ , blue points  $Q_i$  are coloured black and green points  $Q_i$  are coloured white. For  $l+1 \leq i \leq 2k$ , blue points  $Q_i$  are coloured white and green points  $Q_i$  are coloured black. Points with even index are called even, points with odd index are called odd. Then the following lemma is immediate:

**Lemma 14.** *A path-like changing trail in the two-coloured graph defined above can only connect points of different colours (out of black and white) and of different parity (by Observation 10); e.g., some white  $Q_{2m}$  and some black  $Q_{2n+1}$ .*

Now fix an arbitrary subset of points  $\{Q_{i_1}, \dots, Q_{i_m}\}$ . Start with an arbitrary two-coloured graph from  $s_{\lambda/\mu} s_{\sigma/\tau}$  (interpreted again as the product of the generating functions of the corresponding families of nonintersecting lattice paths) and recolour the changing trails starting in  $Q_{i_1}, \dots, Q_{i_m}$ . In general, this will give another two-coloured graph, which can be interpreted as belonging to some other  $s_{\lambda'/\mu'} s_{\sigma'/\tau'}$ . Take an arbitrary object (i.e., two-coloured graph) from  $s_{\lambda'/\mu'} s_{\sigma'/\tau'}$  and repeat the same recolouring operation as long as it generates some “new” (yet unseen) object.

The set of objects thus generated decomposes into two disjoint sets: One set,  $O_0$ , encompasses all objects which show the same colouring of points  $Q_{i_1}, \dots, Q_{i_m}$  as in the starting object; the other,  $O_1$  encompasses the objects with the opposite colouring for these points.

It is clear that recolouring changing trails which start in points  $Q_{i_1}, \dots, Q_{i_m}$  establishes a bijection between  $O_0$  and  $O_1$ .

On the other hand, each object in  $O_0$  belongs to some  $s_{\lambda''/\mu''}s_{\sigma''/\tau''}$ : Denote the set of all the corresponding quadruples  $(\lambda'', \mu'', \sigma'', \tau'')$  which occur in this sense by  $S_0$ . The same consideration applies to  $O_1$ : Denote by  $S_1$  the corresponding set of quadruples  $(\lambda', \mu', \sigma', \tau')$ .

**Lemma 15.** *Given the above definitions, we have the following “generic” identity for skew Schur functions:*

$$\sum_{(\lambda', \mu', \sigma', \tau') \in S_1} s_{\lambda'/\mu'} s_{\sigma'/\tau'} = \sum_{(\lambda'', \mu'', \sigma'', \tau'') \in S_0} s_{\lambda''/\mu''} s_{\sigma''/\tau''}. \quad (8)$$

This statement is certainly as general as useless: Let us specialize to a somewhat “friendlier” assertion.

**Lemma 16.** *Given the above definitions, assume that all black points have the same parity, and that all white points have the same parity. Then (8) specializes to*

$$s_{\lambda/\mu} s_{\sigma/\tau} = \sum_{(\lambda', \mu', \sigma', \tau') \in S_1} s_{\lambda'/\mu'} s_{\sigma'/\tau'}, \quad (9)$$

where  $S_1$  encompasses all the quadruples  $(\lambda', \mu', \sigma', \tau')$  which correspond to any two-coloured graph object that can be obtained by recolouring the changing trails starting in points  $Q_{i_1}, \dots, Q_{i_m}$  in any “initial” two-coloured graph object from  $s_{\lambda/\mu} s_{\sigma/\tau}$ .

*Proof.* Without loss of generality we may assume that all even points are white and all odd points are black in  $s_{\lambda/\mu} s_{\sigma/\tau}$ . By recolouring changing trails, all the points  $Q_{i_1}, \dots, Q_{i_m}$  are matched with points of opposite colour and parity.

So if  $Q_i$  is odd and black, then the recolouring trail starting at  $Q_i$  connects it with some other point  $Q_k$  which is even and white: After recolouring,  $Q_i$  is odd and white, and the recolouring operation altogether yields some two-coloured graph object belonging to some  $s_{\lambda'/\mu'} s_{\sigma'/\tau'}$ .

Now if we apply the recolouring operation to an *arbitrary* object from  $s_{\lambda'/\mu'} s_{\sigma'/\tau'}$ , the only possible partners for “wrongly-coloured”  $Q_i$  (odd, but white) is another “wrongly-coloured”  $Q_j$  (even, but black). Hence this operation takes objects from  $s_{\lambda'/\mu'} s_{\sigma'/\tau'}$  back to  $s_{\lambda/\mu} s_{\sigma/\tau}$ .  $\square$

## 6. PROOF OF THE PLÜCKER RELATIONS

In order to show that the general assertions of Section 5 do in fact lead to some interesting identities, we give a proof of the Plücker relations (Theorem 5), which is based on Lemma 16.

*Proof.* In the notation of Section 5, let

$$\lambda = (2n(n-1), 2(n-1)^2, \dots, 4(n-1), 2(n-1))$$

and

$$\sigma = ((2n-1)(n-1), (2n-3)(n-1), \dots, 3(n-1), n-1),$$

$\mu = \tau = (0, \dots, 0)$ ; and choose horizontal offset  $t = 0$ . I.e., interpret  $s_\lambda s_\sigma$  as the generating function of two-coloured graph objects consisting of two  $n$ -tuples of nonintersecting lattice paths, coloured green and blue, respectively, where green path  $P_i^g$  starts at  $(-i, 1)$  and ends at  $(\lambda_i - i, N)$ , and where blue path  $P_i^b$  starts at  $(-i, 1)$  and ends at  $(\sigma_i - i, N)$ .

Observe that this setting obeys the assumptions of Lemma 16.

Now consider the set of green endpoints  $\{Q_1, \dots, Q_k\}$ , where  $Q_i = (\lambda_{r_i} - r_i, N)$ . (Here,  $1 \leq r_1 < r_2 < \dots < r_k \leq n$  is the fixed list of integers from Theorem 5.) Recolouring changing trails which start at these points amounts to determining the set  $\{R_1, \dots, R_k\}$  of respective endpoints of the changing trails, and changing colours.

Assume that  $R_i = (\sigma_{s_i} - s_i, N)$ , then in terms of the associated Schur functions Lemma 16 directly leads to the identity:

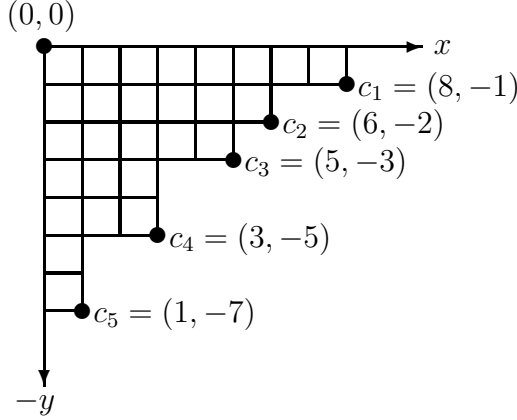
$$s_\lambda s_\sigma = \sum_{1 \leq s_1 < \dots < s_k \leq n} s_{(\lambda_1, \dots, \sigma_{s_1}, \dots, \sigma_{s_k}, \dots, \lambda_n)} s_{(\sigma_1, \dots, \lambda_{r_1}, \dots, \lambda_{r_k}, \dots, \sigma_n)}, \quad (10)$$

where the notation of the summands means that parts  $\lambda_{r_i}$  were exchanged with parts  $\sigma_{s_i}$ , respectively.

By the Jacobi–Trudi identity (4) and Observation 4, (5) and (10) are in fact equivalent.  $\square$

**Remark 17.** *In fact, even the quite general assertion of Lemma 15 can be generalized further: So far, our lattice paths always had starting points and end points at the same horizontal lines  $(., 1)$  and  $(., N)$ , corresponding to the range of variables  $x_1, \dots, x_N$ . Dropping this constraint yields Schur functions with different ranges of variables (e.g.,  $s_\lambda(x_4, x_5, x_6)$ ). Recalling that (see Remark 13) we actually also do allow partitions of different lengths, it is easy to see that Theorem 5 in [12] (which is a generalization of Ciucu’s Schur function identity (6)) can be proved in the same way as Lemma 15.*

FIGURE 7. Illustration of outer corners and special drawing of Ferrers board for partition  $\lambda = (8, 6, 5, 3, 3, 1, 1)$ .



## 7. KLEBER'S THEOREM

The theorem [11, Thm. 3.2] is expressed in terms of certain operations on Ferrers boards (called Young diagrams in [11]): In order to state it, we need to describe the relevant notation.

First, we introduce a particular way of drawing the Ferrers board of  $\lambda = (\lambda_1, \dots, \lambda_r)$  in the plane: Let  $x_1 > x_2 > \dots > x_n > x_{n+1} = 0$  be the ordered list of the *distinct* parts contained in  $\lambda$ ; set  $y_i =$  the number of parts of  $\lambda$  which are  $\geq x_i$ .

Setting  $y_0 = 0$ , we have  $0 = y_0 < y_1 < \dots < y_n$ , and  $(x_i), (y_i)$  simply yield another encoding of the partition  $\lambda$ :

$$\lambda = (x_1^{y_1 - y_0}, x_2^{y_2 - y_1}, \dots, x_n^{y_n - y_{n-1}}).$$

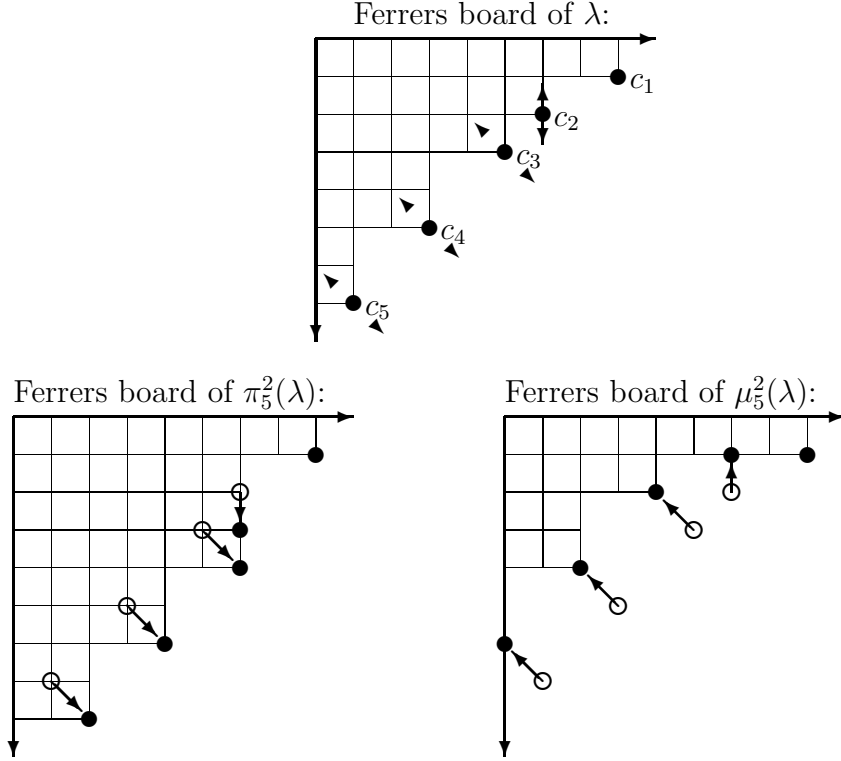
Now consider the  $n$  points  $(x_1, -y_1), (x_2, -y_2), \dots, (x_n, -y_n)$  in the plane: The Ferrers board of  $\lambda$  is represented as the set of points  $(x, -y)$  such that:

$$\begin{aligned} x &\geq 0 \text{ and } y \geq 0, \\ x &\leq x_i \text{ and } y \leq y_i \text{ for some } i. \end{aligned}$$

Figure 7 illustrates this concept. The  $n$  points  $c_1 = (x_1, -y_1), c_2 = (x_2, -y_2), \dots, c_n = (x_n, -y_n)$  are called *outside corners*, the  $n+1$  points  $(x_1, -y_0), (x_2, -y_1), \dots, (x_{n+1}, -y_n)$  are called *inside corners*.

Now we are in a position to define two operations on partitions: In the above notation, take two integers  $i, j$  such that  $1 \leq i \leq j \leq n$  and define two partitions derived from the original  $\lambda$  via manipulating the

FIGURE 8. Illustration of operations  $\pi_j^i$  and  $\mu_j^i$  for  $i = 2$ ,  $j = 5$  applied to  $\lambda = (8, 6, 5, 3, 3, 1, 1)$ .



inside and outside corners of its associated Ferrers board:

$\pi_j^i(\lambda)$  : add 1 to each of  $x_{i+1}, \dots, x_j; y_i, \dots, y_j$ ,

$\mu_j^i(\lambda)$  : add  $-1$  to each of  $x_{i+1}, \dots, x_j; y_i, \dots, y_j$ .

These operations add or remove, respectively, a *border strip* that reaches from the  $i$ -th outside corner to the  $j$ -th inside corner (see Figure 8).

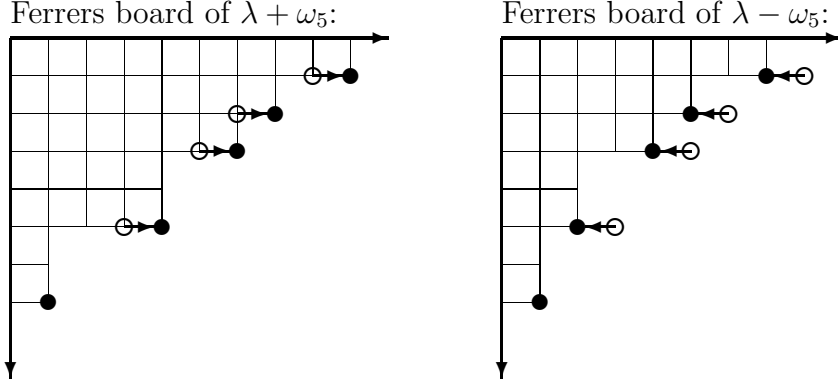
We need to add or remove *nested border strips*: Given integers  $1 \leq i_1 < \dots < i_k \leq j_k < \dots < j_1 \leq n$ , we define

$$\pi_{j_1, \dots, j_k}^{i_1, \dots, i_k} = \pi_{j_1}^{i_1} \circ \dots \circ \pi_{j_k}^{i_k},$$

$$\mu_{j_1, \dots, j_k}^{i_1, \dots, i_k} = \mu_{j_1}^{i_1} \circ \dots \circ \mu_{j_k}^{i_k}.$$

Note that the corners which are shifted by these operations might not appear as corners in the geometric sense any more; nevertheless we consider them as the object for subsequent operations  $\pi$  and  $\mu$ : Nesting

FIGURE 9. Illustration of operation  $\lambda \pm \omega_l$  for  $l = y_4 = 5$ , applied to  $\lambda = (8, 6, 5, 3, 3, 1, 1)$ .



$\pi$  and  $\mu$  in this sense yields something which can be interpreted again as a partition, since we always have  $x_i \geq x_{i+1}$  and  $y_i \leq y_{i+1}$  (see Figure 8.)

The last operation we need is the following: In the above notation, let  $k$  be an integer,  $1 \leq k \leq n$ . Clearly, the Ferrers board contains at least one column of length  $l = y_k$ : Adding or removing some column of length  $l$  amounts to adding  $\pm 1$  to all coordinates  $x_i$ ,  $1 \leq i \leq k$ . We denote this operation by  $\lambda \pm \omega_l$ . (See Figure 9.)

**Theorem 18** (Theorem 3.2 in [11]). *Let  $\lambda = (\lambda_1, \lambda_2, \dots, \lambda_r)$  be a partition with  $n$  outside corners. For an arbitrary integer  $k$ ,  $1 \leq k \leq n$ , set  $l = y_k$  (in the above notation). Then we have:*

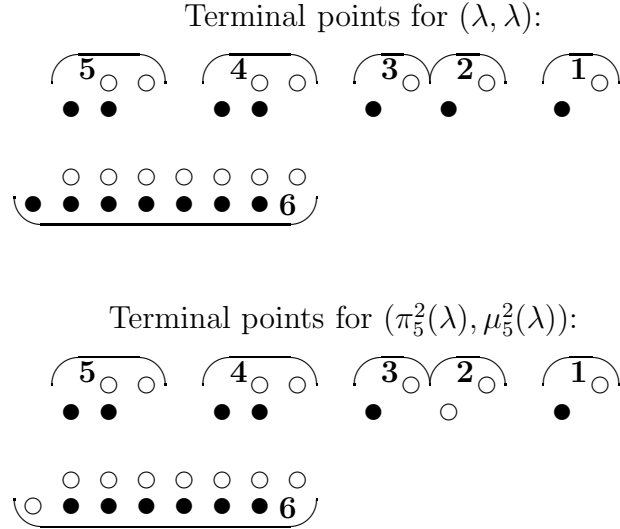
$$s_\lambda s_\lambda = s_{\lambda + \omega_l} s_{\lambda - \omega_l} + \sum_{m \geq 1} \sum_{\substack{1 \leq i_1 < \dots < i_m \leq k \\ k \leq j_m < \dots < j_1 \leq n}} (-1)^{m-1} s_{\pi_{j_1, \dots, j_m}(\lambda)} s_{\mu_{j_1, \dots, j_m}(\lambda)}. \quad (11)$$

The connections between Ferrers boards and nonintersecting lattice paths were illustrated in Section 3: Here we have to give the proper “translation” of operations  $\pi_j^i$  and  $\mu_j^i$  to nonintersecting lattice paths.

First observe that the outside corners of a partition correspond to *blocks of consecutive endpoints* (here, consecutive means “having distance 1 in the horizontal direction”) in the lattice path interpretation: Number these blocks from right to left by  $1, 2, \dots, n$ , and denote the additional block of (consecutive) starting points by  $n+1$  (see the upper picture in Figure 10).

Interpret some object from  $s_\lambda s_\lambda$  in the same way as in Section 5. More precisely, let  $\sigma = \lambda$ ,  $\mu = \tau = 0$  and horizontal offset  $t = 1$  in

FIGURE 10. Illustration of operations  $\pi_j^i$  and  $\mu_j^i$  for  $i = 2, j = 4$  applied to  $\lambda = (8, 6, 5, 3, 3, 1, 1)$ , translated to lattice paths.



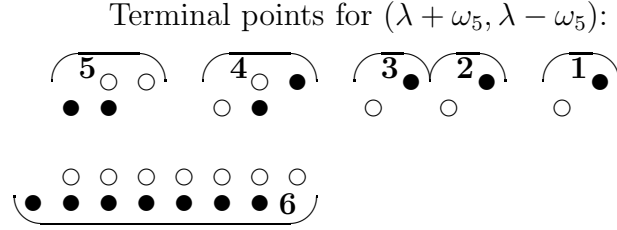
the general definitions preceding Lemma 15. Figure 10 illustrates the position of starting points and end points of the corresponding lattice paths: Blue points are drawn as black dots, green points are drawn as white dots; blocks are indicated by horizontal braces.

It is easy to see that the simultaneous application of  $\pi_j^i$  to the “green object” and of  $\mu_j^i$  to the “blue object” amounts to interchanging colours of the leftmost point in blue block  $i$  and of the appropriate endpoint of a corresponding changing trail in block  $j + 1$  (i.e., the rightmost point in green block  $j + 1$  if  $j < n$ , or the leftmost point in blue block  $n + 1$  if  $j = n$ ; see Figure 10).

Likewise, adding some column of height  $l = y_k$  to the “blue object” and simultaneously removing such column from the “green object” amounts to interchanging colours of the leftmost blue point and the rightmost green point in blocks  $1, 2, \dots, k$  if  $k < n$ ; if  $k = n$ , then the same effect can be achieved by interchanging colours of the leftmost blue point and the rightmost green point in block  $n + 1$ . (See Figure 11.)

*Proof of Theorem 18:* Consider a two-coloured object from  $s_\lambda s_\lambda$  in the lattice path interpretation. As in Section 5, we look at the noncrossing perfect matching that the changing trails induce among their  $2n + 2$

FIGURE 11. Illustration of operations  $\lambda \pm \omega_l$  for  $l = y_4 = 5$ , applied to  $\lambda = (8, 6, 5, 3, 3, 1, 1)$ , translated to lattice paths.



endpoints, the leftmost and rightmost points in blocks  $1, \dots, n, n+1$ . Note that in the case of  $s_\lambda s_\lambda$ , the parity constraint and the colour constraint of Lemma 14 coincide.

Now consider the  $k$  changing trails which begin at the leftmost (blue) endpoints of blocks  $1, 2, \dots, k$ . There are exactly two cases:

- (1) The changing trails match these points up with the rightmost (green) endpoints of blocks  $1, 2, \dots, k$ : Then recolouring these  $k$  trails results in an object of type  $s_{\lambda+\omega_l} s_{\lambda-\omega_l}$ . Conversely, given an object of type  $s_{\lambda+\omega_l} s_{\lambda-\omega_l}$ , the parity and colour constraints of Lemma 14 force the points in blocks  $1, 2, \dots, k$  to be matched amongst themselves, so they are in bijection with this subset of  $s_\lambda s_\lambda$  objects.
- (2) Otherwise, some of those  $k$  points must match up with points in blocks  $k+1, \dots, n, n+1$ . Suppose there are  $m$  such matchings, and that they match the leftmost points in blocks  $i_1 < i_2 < \dots < i_m$  with points in blocks  $j_1 > j_2 > \dots > j_m$ . (Since the changing trails cannot cross, we in fact know that  $i_r$  is matched with  $j_r$ , for  $1 \leq r \leq m$ .) Recolouring these  $m$  trails gives an object of type  $s_{\pi_{j_1 \dots j_m}^{i_1 \dots i_m}}(\lambda) s_{\mu_{j_1 \dots j_m}^{i_1 \dots i_m}}(\lambda)$ .

This time, though, we do not have a bijection. Given an object of  $s_{\pi_{j_1 \dots j_m}^{i_1 \dots i_m}}(\lambda) s_{\mu_{j_1 \dots j_m}^{i_1 \dots i_m}}(\lambda)$ , the same parity and colour constraints of Lemma 14 do guarantee that  $m$  changing trails connect each  $i_r$  with  $j_r$ . However, when we recolour them to get an object of  $s_\lambda s_\lambda$ , we may arrive at an object that has *other* changing trails leaving blocks  $1, \dots, k$ , aside from the  $m$  we considered.

Thus, we are in the “typical” situation for an inclusion–exclusion argument, which immediately yields equation (11).

This finishes the proof.  $\square$

**Remark 19.** *When  $k = 1$ , both cases of the above proof amount to recolouring the trail beginning at the rightmost green endpoint, so this is a special case of Lemma 16. The  $k = n$  case follows similarly, after exchanging blue and green.*

## REFERENCES

- [1] D. BRESSOUD, Proofs and Confirmations: The Story of the Alternating Sign Matrix Conjecture, Cambridge University Press, New York, 1999.
- [2] C. L. DODGSON, Condensation of Determinants, Proceedings of the Royal Society of London **15** (1866), 150–155.
- [3] M. FULMEK, A Schur function identity, J. Combinatorial Theory A **77** No. 1 (1997).
- [4] M. FULMEK AND C. KRATTENTHALER, Lattice path proofs for determinant formulas for symplectic and orthogonal characters, J. Combinatorial Theory A **77** (1997), 3–50.
- [5] W. FULTON AND J. HARRIS, Representation Theory, Springer, New York, 1991.
- [6] I. M. GESSEL AND X. VIENNOT, Determinants, paths, and plane partitions, preprint, 1988.
- [7] I. P. GOULDEN, Quadratic Forms of Skew Schur Functions, European J. of Combinatorics, **9** (1988), 161–168.
- [8] A. HAMEL, private communication, 1997.
- [9] C.G.J. JACOBI, De formatione et proprietatibus Determinantium, in: Gesammelte Werke, vol. 3, Georg Reimer, Berlin (1884), 355–392; first published in Journal für Reine und Angewandte Mathematik **22** (1841), 285–318.
- [10] A. N. KIRILLOV, Completeness of states of the generalized Heisenberg magnet. (Russian), Zap. Nauchn. Sem. Leningrad. Otdel. Mat. Inst. Steklov. (LOMI) **134** (1984), transl. in J. Soviet Math. **36** (1987), 115–128.
- [11] M. KLEBER, Plücker Relations on Schur Functions, Journal of Algebraic Combinatorics, to appear.
- [12] C. KRATTENTHALER, Schur Function identities and the number of perfect matchings of holey Aztec rectangles, in: “ $q$ -series from a Contemporary Perspective”, M.E.H. Ismail, D. Stanton, eds., Contemporary Math. **254**, Amer. Math. Soc., Providence, R.I., 2000, 335–350.
- [13] I. G. MACDONALD, Symmetric Functions and Hall Polynomials, Oxford University Press, New York/London, 1979.
- [14] T. MUIR, The theory of determinants in the historical order of development, 4 vols., Macmillan, London, 1906–1923.
- [15] J. PROPP AND R. P. STANLEY, Domino tilings with barriers, J. Combinatorial Theory (A) **87** (1999), 347–356.
- [16] B. E. SAGAN, The symmetric group, Wadsworth & Brooks/Cole, 1991.
- [17] R. P. STANLEY, Theory and applications of plane partitions: Part 1,2, Stud. Appl. Math **50** (1971), 167–188, 259–279.
- [18] R. P. STANLEY, Enumerative Combinatorics, Vol. 2, Cambridge Studies in Advanced Mathematics **62**, Cambridge University Press, 1999.

- [19] D. STANTON AND D. WHITE, Constructive Combinatorics, Undergraduate Texts in Math., Springer-Verlag New York, Berlin, Heidelberg, Tokyo, 1986.
- [20] J. R. Stembridge, *Nonintersecting paths, pfaffians and plane partitions*, Adv. Math. **83** (1990), 96–131.
- [21] B. STURMFELS, Algorithms in Invariant Theory, Texts and Monographs in Symbolic Computation, Springer-Verlag, Wien, (1993).
- [22] H.W. TURNBULL, The Theory of Determinants, Matrices, and Invariants, Dover Publications, New York, (1960).
- [23] D. ZEILBERGER, Dodgson's Determinant-Evaluation Rule proved by TWO-TIMING MEN and WOMEN, Elect. J. of Combinatorics **4**(2) [Wilf Festschrift volume], 1997.
- [24] D. ZEILBERGER, A combinatorial approach to matrix algebra, Discrete Math. **56**, (1985), 61–72.

INSTITUT FÜR MATHEMATIK DER UNIVERSITÄT WIEN, STRUDLHOFGASSE 4,  
A-1090 WIEN, AUSTRIA.

MASSACHUSETTS INSTITUTE OF TECHNOLOGY, 77 MASSACHUSETTS AVENUE,  
CAMBRIDGE, MA 02139, USA.

*E-mail address:* Markus.Fulmek@Univie.Ac.At, Kleber@Math.Mit.Edu